

A Theory of Cooperative Diffusion in Dense Granular Flows

Martin Z. Bazant*

Department of Mathematics, Massachusetts Institute of Technology, Cambridge 02139

(Dated: May 8, 2004)

Dilute granular flows are routinely described by collisional kinetic theory, but dense flows require a fundamentally different approach, due to long-lasting, many-body contacts. In the case of silo drainage, many continuum models have been developed for the mean flow, but no realistic statistical theory is available. Here, we propose that particles undergo cooperative displacements in response to diffusing “spots” of free volume. The typical spot size is several particle diameters, so cages of nearest neighbors tend to remain intact over large distances. The spot hypothesis relates diffusion and cage-breaking to volume fluctuations and spatial velocity correlations, in agreement with new experimental data. It also predicts density waves caused by weak spot interactions. Spots enable fast, multiscale simulations of dense flows, in which a small, internal relaxation enforces packing constraints during spot-induced motion. In the continuum limit of the model, tracer diffusion is described by a new stochastic differential equation, where the drift velocity and diffusion tensor are coupled non-locally to the spot density. The same mathematical formalism may also find applications to glassy relaxation, as a compelling alternative to void (or hole) random walks.

I. INTRODUCTION

In spite of a venerable engineering literature [1, 2, 3], the study of granular materials is attracting a growing community of physicists [4, 5, 6, 7, 8], who sense that basic principles remain to be discovered [9], including “the chance to reinvent statistical mechanics in a new context” [10]. Of course, individual grains obey the laws of classical physics, but in many ways their collective behavior defies standard assumptions in statistical thermodynamics and hydrodynamics. Static properties of random packings, such as geometrical correlation functions [11, 12], the jamming transition [13, 14, 15, 16, 17, 18], and local force distributions [19, 20, 21, 22, 23, 24, 25] are far from fully understood, but granular flows may pose even more fundamental open questions.

Naturally, the most attention has focused on the regime of fast, dilute flow because it is closest to the familiar molecular-fluid state. In this regime, grains undergo simple random walks due to binary (or possibly many-body) collisions, which differ from those in normal fluids only by being inelastic. From these postulates, continuum equations for hydrodynamics and heat transfer can be formally derived from various modifications of Boltzmann’s kinetic theory of gases [26, 27, 28, 29, 30, 31, 32, 33]. Due to inelastic collisions, external forcing must supply enough kinetic energy to approximately satisfy the assumption of thermal equilibrium. The resulting definition of a time-dependent, local “granular temperature” in terms of velocity fluctuations is somewhat controversial, since classical statistical mechanics may break down with inelastic collisions [10]. For example, non-extensive Tsallis statistics [34] can be derived from the simple “inelastic Maxwell model” of a granular gas [35]. In any case, it is clear that kinetic theory breaks

down with increasing density [36, 37], when long-lasting many-body contacts are formed. Due to gravity, such is usually the case in granular materials.

In seeking new and relevant physics, therefore, it seems more fruitful to focus on the opposite regime of slow, dense flow — closer to the “granular solid” than the “granular gas” [6]. Mean flow fields in draining silos, incline chutes, and shear cells have been studied extensively, but a simple unified description remains elusive. Classical continuum models of dense flows are based on plasticity theory from soil mechanics [1, 2]. Although they remain popular in engineering, these models predict complicated patterns of velocity discontinuities (“rupture surfaces”), consistent with some experiments [38, 39, 40] but not others [37, 41, 42, 43, 44], and can lead to violent instabilities [45, 46]. On the other hand, another class of early models for silo drainage (discussed below in section) involves only simple geometrical considerations [43, 47, 48, 49, 50, 51]. Recent attempts to develop continuum models for dense flows have introduced a remarkable variety of physical postulates, such as a temperature-dependent viscosity [52], density-dependent viscosity [53, 54], non-local stress propagation along hypothetical arches [55], self-activated shear events due to non-local stress fluctuations [56, 57], coexisting liquid and solid micro-phases governed by a Landau-like order parameter [58, 59], and shear-induced local rearrangements mediated by free-volume kinetics [60, 61].

Putting aside the question of which of these continuum models best describes the mean velocity, we focus here on the stochastic motion of individual particles outside the collisional regime, for which no theory is available. Even in experiments, little attention has been paid to this fundamental issue, perhaps due to the practical difficulty of tracking individual particles in dense flows. Due to recent advances in digital video imaging, however, thousands of particles near the wall of a dense granular flow can now be tracked simultaneously with very high resolution [37, 62, 63] (well beyond previous stan-

*Electronic address: bazant@math.mit.edu

dards [36, 41, 64]). Combining these techniques with magnetic resonance imaging and x-ray tomography can also yield three-dimensional information [65]. Complete microscopic motion in the bulk can also be obtained from granular dynamics simulations, now involving up to hundreds of thousands of particles in three dimensions [23, 66, 67, 68, 69, 70]. These revolutionary capabilities should aid in developing a statistical theory of dense granular flows.

In some sense, work along these lines has already begun with attempts to define a meaningful temperature for dense granular systems. The notion of “Edwards temperature” [71, 72, 73], analogous to structural temperatures in glasses [74], has attracted increasing attention over the past decade. The Edwards temperature differs from its Boltzmann counterpart in that the entropy is based on static random packings at a given volume, rather than thermal configurations at a given energy. As such, it may be related to the compaction of powders under vibration [71, 75]. Some support for the idea has come from recent molecular dynamics simulations verifying an effective Einstein relation between mobility and diffusivity in an artificial shear flow [67]. Nevertheless, it is not clear how the Edwards equilibrium ensemble relates to hydrodynamics and diffusion (if at all) since no analog of the Boltzmann equation of kinetic theory has been proposed. This would seem to require replacing the usual hypothesis of a random walk, due to ballistic motion between instantaneous collisions, with a new dynamical mechanism.

Thus we arrive at the central question of this work:

Is there a simple analog of the random walk for a dense granular flow?

Roughly a century after random-walk theory was first developed, the original idea of a single entity, such as a mosquito [76], sound-wave amplitude [77, 78], Brownian particle [79, 80], or stock price [81], undergoing random displacements remains in most subsequent generalizations [82, 83, 84]. For example, the “continuous-time random walk” of Montroll and Weiss [85, 86] and related models [83], which describe anomalous diffusion in semi-conductors [87], turbulent flows [88] and many other systems [89] via a random waiting time between steps, also assume an independent random walker, unaffected by its neighbors. The same is true of the “persistent random walk” of Fürth [90] and Taylor [91] which introduces auto-correlations between steps, e.g. to model a transition from short-time ballistic to long-time diffusive motion [92, 93].

Of course, there are correlations between different random walkers in any condensed-matter system (or financial market [84]), but in most cases it is reasonable to assume that the diffusion of a single particle is independent of all the others. This universal independence of single-particle trajectories is often related to attaining the thermodynamic limit, in which an enormous number ($N \approx 10^{23}$) of particles undergo very frequent collisions

($\omega = 10^{14}$ Hz) at finite temperature (in the classical sense). As a result, short-range many-body interactions have little effect on tracer diffusion at macroscopic length and time scales, aside from influencing parameters, such as the diffusivity.

In stark contrast, the “cages” of neighboring particles in a dense granular material may remain at least partially intact for the entire duration of slow flow [37], due to strong internal energy dissipation and much smaller system sizes (e.g. $N \approx 10^5$). Even at macroscopic length and time scales, therefore, particles must diffuse together in a cooperative fashion, and it is not clear what kind of statistics might describe their collective motion. Boltzmann’s kinetic theory of gases does not appear to be the appropriate starting point.

In this article, we propose a simple mathematical model for cooperative diffusion and apply it to slow granular drainage from a silo, as shown in Fig. 1. After summarizing our results in section II, we begin by showing that the only existing model for granular diffusion, based on the concept of diffusing voids, is fundamentally flawed and draw clues from experiments as to what could be missing. In section IV, we introduce the general concept of a “spot” of cooperative diffusion, and in section V we show that it suffices to predict a wide variety of experimental data. In section VI, we briefly discuss Monte Carlo simulations with the model and spot-based multi-scale algorithms. In section VII, we derive general continuum equations for tracer diffusion in the spot model, focusing in section VIII on the case of granular drainage. We conclude in sections IX–XI by discussing how the theory might have broad applicability to cooperative diffusion in amorphous materials.

II. SUMMARY OF RESULTS

As a guide for the reader, we list our main results:

1. A new microscopic picture of dense granular flows is presented in Figs. 6 and 7. Rising spots of free volume cause strongly correlated random displacements of blocks of neighboring particles. Each random spot path corresponds to a thick chain of repeating particles.
2. In section IV, simple calculations show how the spot hypothesis resolves the “paradox of granular diffusion” illustrated in Fig. 1: Particles diffuse several orders of magnitude more slowly than free volume.
3. In section V, predictions of the Péclet number, diffusion length, and cage-breaking distance, consistent with experimental data, are made by assuming volume fluctuations of order one percent. The vertical diffusion length of free volume, which is difficult to measure experimentally, is also predicted.

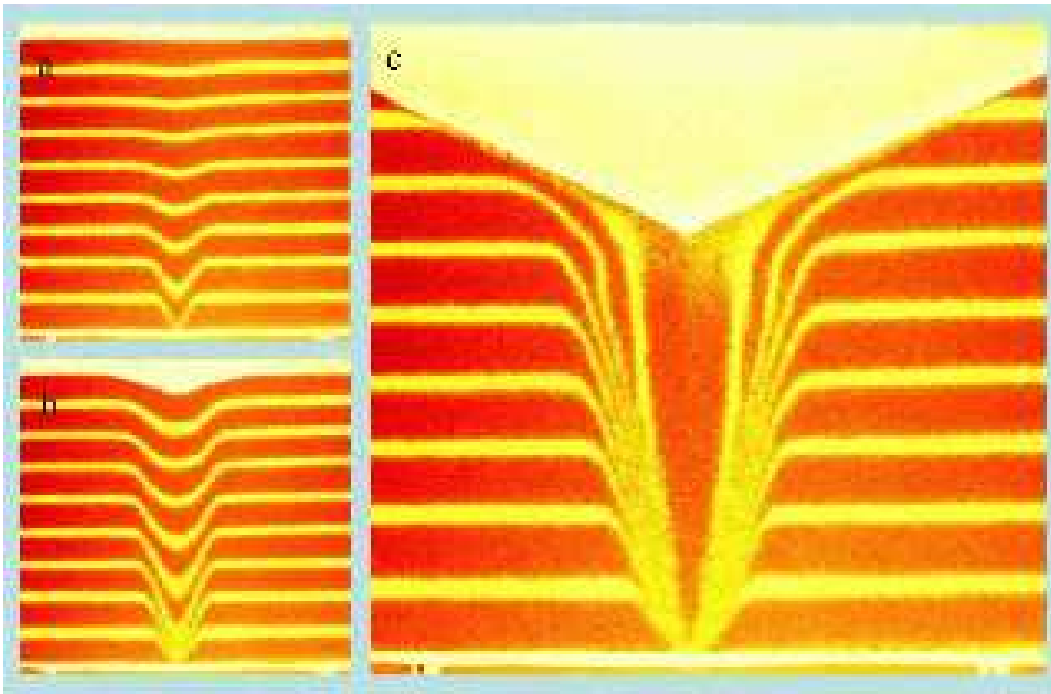


FIG. 1: Sequence of experimental photographs of a $d = 3\text{mm}$ glass beads draining from a quasi-two-dimensional silo (courtesy of A. Samadani and A. Kudrolli [42]). Particles are colored according to their initial positions in equally spaced horizontal layers when the flow began.

4. Direct experimental evidence for spots, through spatial velocity correlations, is shown in Fig. 8.
5. The necessity of weak repulsive interactions between spots naturally explains experimental density waves, sketched in Fig. 9, which propagate upward in wide funnels and possibly downward in narrow funnels.
6. Monte Carlo simulations with the simplest version of the model, shown in Figs. 10 and 11, accurately describe tracer-particle dynamics and some aspects of many-body correlations, although unphysical density fluctuations grow in regions of high shear.
7. The density may be stabilized by minor relaxations within spots to enforce packing constraints, which amounts to a very efficient multiscale simulation algorithm for granular flow. These extra fluctuations, sketched in Fig. 12, may be responsible for the nontrivial (sub-ballistic) super-diffusion seen in experiments at scales less than a particle diameter.
8. In section VII, the mean-field continuum limit of the model is analyzed, starting from non-local stochastic differential equation, Eq. (28). The result is a Fokker-Planck equation for tracer diffusion, Eq. (30), whose coefficients in Eqs.(33) and (37) are coupled non-locally to the spot (or free-volume) density.

9. A general tensor relation between transport coefficients, Eqs. (40), is derived, which relates spatial velocity correlations and the diffusivities of particles and free volume.

III. TOWARDS A STATISTICAL THEORY

A. The Kinematic Model for the Mean Velocity

In the 1970s, engineers developed a very simple “Kinematic Model” for the mean velocity field in a steadily draining silo [1], such as the flow illustrated in Fig. 1. It is based on the following constitutive law, suggested by Nedderman and Tuzun [43],

$$\mathbf{u} = b \nabla_{\perp} v \quad (1)$$

which postulates that the horizontal velocity, \mathbf{u} , is proportional to the horizontal gradient, ∇_{\perp} , of the downward velocity component, v (i.e. the shear rate). We refer to the constant of proportionality, b , as the “diffusion length” of free volume for reasons soon to become clear. The intuition behind this relation is that particles should tend to drift horizontally toward regions of faster downward flow, which are less dense and more accommodating of newcomers. Assuming that these density fluctuations are small enough to justify steady-state incompressibility

yields an equation for the downward velocity,

$$\frac{\partial v}{\partial z} = b \nabla_{\perp}^2 v, \quad (2)$$

which is simply the diffusion equation, where the vertical coordinate, z , plays the role of time. As such, “initial conditions” must be specified for the downward velocity at the bottom of the silo, and information propagates upward.

For example, a point source of velocity (a narrow orifice) at $z = 0$ in a quasi-two dimensional silo produces the basic solution,

$$v(x, z) = \frac{e^{-x^2/4bz}}{\sqrt{4\pi bz}} \quad (3)$$

for the case of constant b . The flow is effectively confined to a region of parabolic streamlines due to the diffusive scaling, $\Delta x \propto \sqrt{z}$. As shown in Fig. 1, this prediction is in rather good agreement with experimental measurements of the bulk flow (well below the free surface) for large, dry grains [37, 41, 42, 44, 47]. (For fine powders and soils, the model breaks down, presumably due to cohesion between grains and/or the influence of the interstitial fluid [1, 44].)

The fact that a single fitting parameter, b , suffices to reproduce the entire flow field reasonably well should be viewed as a major success of the Kinematic Model. Nevertheless, the model fell from favor in the 1980s, in part because the diffusion length seems hard to predict *a priori*. Although b is consistently on the order of a several particle diameters, its precise value depends somewhat on the particle size and flow symmetry [1]. (It also varies with the humidity in cases outside the pure “granular” regime [42].) A Gaussian fit to the downward velocity profile also seems to require a larger value of b in the upper region of the silo, where the flow is more plug-like. This was also seen as problematic, although the model does not really require that b be a constant.

Perhaps a deeper reason for the dissatisfaction with the Kinematic Model is the natural prejudice against a theory seemingly devoid of “physics”. The model depends only upon geometry, via the diffusion length and the silo shape, and not on any of the usual physical variables, such as momentum, mass, energy, temperature, stress, etc. In contrast, more complicated models from soil mechanics involve a stress-based yield criterion, which generally leads to bulk discontinuities in stress and velocity (“rupture zones”) [1, 33]. It is not clear that these models provide a better overall description of silo drainage, but in any case it seems worth taking a fresh look at the simpler Kinematic Model and its possible microscopic justification.

B. The Void Model for the Mean Velocity

Although Nedderman and Tuzun introduced the macroscopic view of Equation (1) as a constitutive relation and Eq. (2) as conservation law [43], both equations

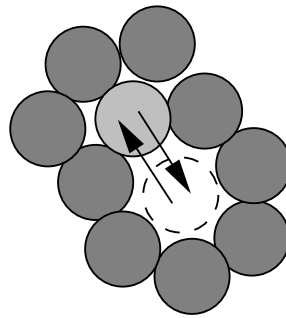


FIG. 2: The Void Hypothesis I. A single particle drops independently from one available cage to another [48, 49, 50] by (equivalently) exchanging with a rising void [47, 51, 97]. As a result, cage breaking occurs at the scale of the particle diameter.

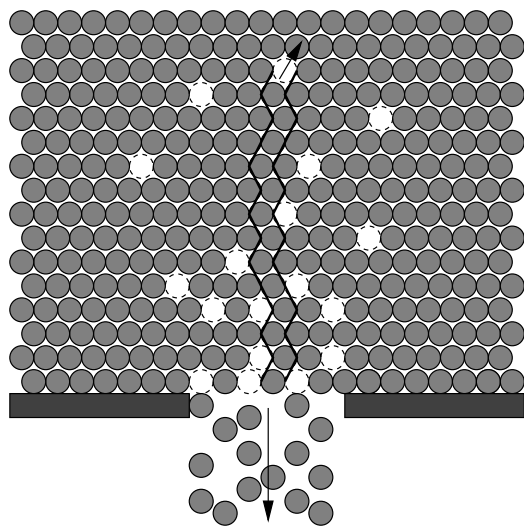


FIG. 3: The Void Hypothesis II. On a lattice [97], a void trajectory emanating from the orifice causes a reptating chain of downward particle displacements (thick lines), each at the scale of the particle diameter.

had been derived years earlier by Litwiniszyn [48, 49, 50] and Mullins [47, 51] from a statistical model which remains, to this day, the only microscopic description of silo drainage. The basic hypothesis is sketched in Figure 2. Litwiniszyn first suggested in 1958 that individual hard-sphere particles diffuse downward through a fixed array of available “cages”, which yields the Kinematic Model for the mean velocity in the continuum limit [48, 49, 50].

Independently, Mullins in 1972 derived the Kinetic Model from the hypothesis that particles move passively downward in response to the upward diffusion of “voids” emanating from the silo orifice [47, 51]. Although formally equivalent to Litwiniszyn’s particle-based model [94], Mullins’ void-based model introduces a fundamentally different perspective, analogous to vacancy diffusion in crystalline solids, which we will find

quite suggestive. (Note that the same mechanism of “hole diffusion” was first proposed in the free-volume theory of molecular liquids and glasses [95, 96], discussed below in section X.)

The Kinematic Model is easily derived from the continuum limit of the Void Model, assuming that voids do not interact. According to the Central Limit Theorem [83], the void concentration, ρ_v , (or probability density) tends toward a Gaussian profile satisfying the diffusion equation,

$$\frac{\partial \rho_v}{\partial z} = b \nabla_{\perp}^2 \rho_v, \quad (4)$$

where the parameter, b , is well-defined microscopic quantity, the void diffusion length (usually assumed to be constant). The mean particle velocity,

$$\rho_p(\mathbf{u}, -v) = -v_0 (-b \nabla_{\perp} \rho_v, \rho_v), \quad (5)$$

is obtained by equating the particle flux density (on the left) with minus the void flux density (on the right), where v_0 is the mean upward drift velocity of the voids (related to the flow rate), and ρ_p is the particle density, which is roughly constant in a dense flow. Equations (1) and (2) follow from Equations (4) and (5).

When physicists, Hong and Caram, revisited the Void Model in 1991, they performed computer simulations of voids undergoing directed random walks on a lattice [97], as illustrated in Fig. 3. Although they did not perform any mathematical analysis, the void diffusion length is easily calculated for any regular lattice:

$$b = \frac{\text{Var}(\Delta \mathbf{x}_v)}{2d_h \Delta z_v} \quad (6)$$

where $\Delta \mathbf{x}_v$ is the random horizontal displacement (in $d_h = 2$ horizontal dimensions) when a void moves up by Δz_v . For example, assuming isotropic transition probabilities to nearest-neighbor sites in the next lattice plane upward, we find $b = d/4\sqrt{6}$ for the face-centered cubic and hexagon close-packed lattices and $b = d/4\sqrt{2}$ for the body-centered cubic lattice. More generally, for any conceivable lattice approximating the random close packing of hard spheres, the Void Model predicts $b \ll d$, in contrast to experimental measurements which always yield $b > d$, e.g. $b = 1.3d$ [37], $b = 2.3d$ [43], $b = 3.5d$ [42], and $b = 2d - 4d$ [41]. This suggests that the microscopic picture of the Void Model is somehow flawed, even though the mean velocity profile is quite reasonable.

C. Particle Dynamics in the Void Model

More serious problems with the Void Model become apparent when one considers diffusion and mixing, which it seems has not previously been done. Mullins and Litwiniszyn were content to use the Void Model as simply a means to derive the continuum equation (2). Likewise,

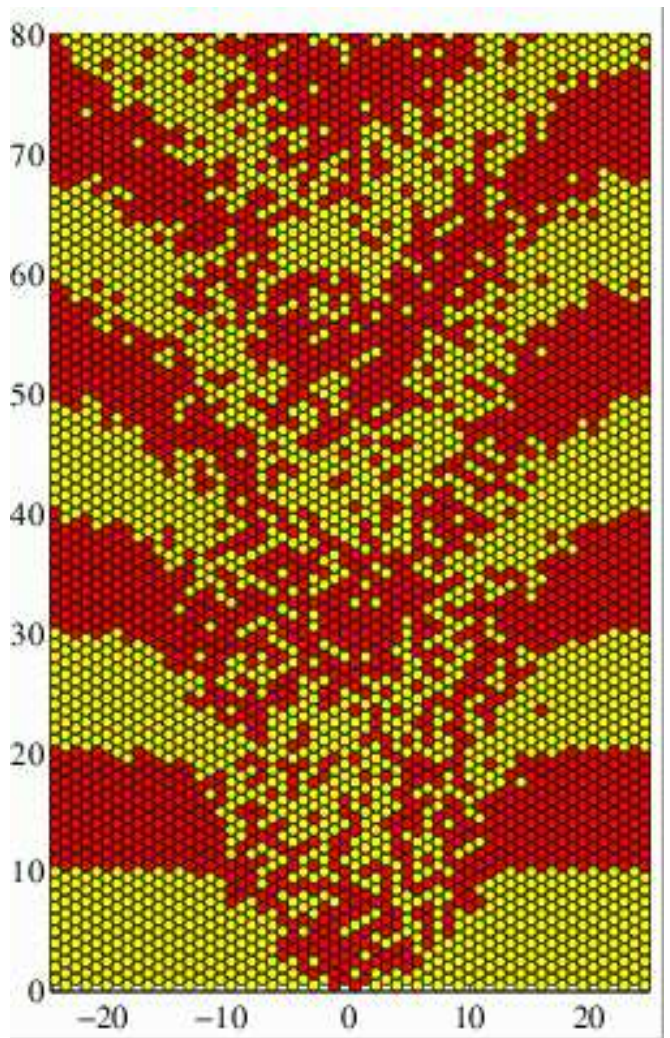


FIG. 4: Simulation of the experiment in Fig. 1 using the Void Model on a triangular lattice, which results in far too much mixing. (Courtesy of Chris Rycroft.)

in spite of doing discrete simulations, Hong and Caram only measured the mean velocity profile.

To quantify the diffusion of particles, we consider geometrical single-particle propagator, $\mathcal{P}_p(\mathbf{x}|z, \mathbf{x}_0, z_0)$, the conditional probability density of finding a particle at horizontal position, \mathbf{x} , after it has fallen to a vertical position, z , from an initial position, (\mathbf{x}_0, z_0) . For a steady mean concentration of voids on a lattice, $\rho_v(\mathbf{x}, z)$, it is straightforward to take the continuum limit of the exact lattice dynamics (as will be described elsewhere) to obtain a partial differential equation for $\mathcal{P}_p(\mathbf{x}|z, \mathbf{x}_0, z_0)$ at length scales much larger than the particle diameter:

$$-\frac{\partial \mathcal{P}_p}{\partial z} = b \nabla_{\perp} \cdot (\nabla_{\perp} \mathcal{P}_p + \mathcal{P}_p \nabla_{\perp} \log \rho_v). \quad (7)$$

This equation may also be derived heuristically as follows. In a uniform flow ($\rho_v = \text{constant}$), a particle does a directed random walk downward with precisely the same

diffusion length as the voids going upward. As in Eq. (4) for the void concentration, this yields the first two terms in Eq. (7), i.e. the diffusion equation with “ $-z$ ” acting like “time”. In a nonuniform flow, the third term represents a horizontal bias of the particle random walk to climb the horizontal gradient of the void concentration, which ensures that the propagator is eventually localized on the source of voids (the silo orifice). The “advection velocity”, $b\nabla_{\perp} \log \rho_v$, is given by the ratio of (minus) the horizontal void flux to vertical void flux, $b\nabla_{\perp} \rho_v / \rho_v$, according to the right hand side of Eq. (5). The task of characterizing solutions to the new equation (7) is left for future work.

D. The Paradox of Granular Diffusion

Here, it suffices to note that the particle dynamics in the Void Model is firmly contradicted by experiments. In a uniform flow, Equation (7) predicts that particles follow statistically identical geometrical trajectories while falling as voids do while rising, with the same diffusion length, b . Figure 1c provides an elegant visual demonstration that this prediction is incorrect. The Void Model would predict that a particle starting near the top of the silo would diffuse horizontally within an inverted parabolic region of the same curvature as the parabolic flow region (set by the diffusion of voids). Therefore, a collection of particles starting near the top of the silo inter-diffuses and mixes across most of the flow region before falling to the middle of the silo, as shown in Fig. 4. Instead, experimental particles mix much less while draining, even in the non-uniform flow region, as the initially sharp interfaces between layers of different colors remain relatively intact during drainage.

The failure of the Void Model has a clear microscopic origin. Particle-tracking experiments on silo drainage (motivated by the theory below) have recently shown that the “cage” of neighbors of a particle is preserved over surprisingly long distances, on the order of hundreds of particle diameters, even comparable to the system size [37]. This experimental result violates the central hypothesis of the Void Model, illustrated in Fig. 2, in any of its forms. On a lattice [97], when a particle moves by interchanging with a diffusing void, it loses roughly half of its neighbors. As this process is repeated, the particle is likely to lose all of its original neighbors after falling by only a few times its own diameter. This quickly results in a rather unphysical degree of mixing, as shown in Figs. 4 and 5.

This same conclusion also applies to the early engineering theories, which are more vague about the microscopic dynamics [1]. Litwiniszyn [48, 49, 50] postulated that particles jump downward from one fixed cage to another, but this implies that a particle completely breaks free of its neighbors with each random displacement. Similarly, Mullins [47, 51, 94] postulated that individual particles move by exchanges with particle-sized voids, indepen-

dently from the random motions of neighboring particles, and this again implies a cage-breaking length comparable to the particle diameter. In reality, particles diffuse in a cooperative fashion, somehow managing to preserve their cages of first neighbors over rather large distances.

How is it possible that the Void Model is able to describe the macroscopic flow while so poorly describing the microscopic dynamics? This illustrates the danger of judging a statistical hypothesis based on only mean quantities, as some authors have argued that the success of the Kinematic Model lends support to the Void Model. The “paradox” of dense granular flow is that the diffusivity of particles is several orders of magnitude smaller than the diffusivity of free volume.

E. More Clues from Experiments

A closer look at experimental images suggests the key to resolving this paradox. As shown in fig. 5(a), an interface between differently colored (but otherwise identical) particles deforms considerably in a non-uniform, dense granular flow, and yet individual particles rarely (if ever) penetrate from one region into the other. This is in stark contrast to diffusion in normal liquids and gases, where the independent random walks of tiny molecules cause an initially sharp interface to become smoothly blurred over time, even in the absence of a flow. Instead, we see that the granular interface in the center panel of Fig. 5 develops some waviness at the scale of several particle diameters. This suggests that particles somehow diffuse *cooperatively* in cage-like blocks, mostly staying together with their nearest neighbors.

This intuitive notion is consistent with other experimental indications of an important length scale of several particle diameters, which is missing in the Void Model. It is well known that a silo will not begin to drain until the orifice is at least several particles wide, and mechanical blocking (due to arching) can occur at somewhat larger orifice widths [1]. The empirical Beverloo correlation [99] implies that the extrapolated outlet diameter where the flow-rate vanishes is roughly 1.5 particle diameters, which has been explained in terms of a controversial empty annulus near the edge of the orifice [3]. For our purposes, the salient point is that a granular material does not drain one particle at a time, so it is impossible to inject individual voids at the orifice. Since packing constraints must be enhanced in the bulk compared to the orifice, it seems highly improbable that voids could form and propagate in the interior of the silo.

On the other hand, if particles tend to preserve their cages while diffusing in the bulk, then they should only pass through the orifice in correlated groups. Particle-tracking measurements of silo drainage show some signs of flow intermittency until the opening is at least six particles wide [37], consistent with the point where the Beverloo correlation becomes acceptable [1]. This again suggests that extended blocks of particles must be allowed

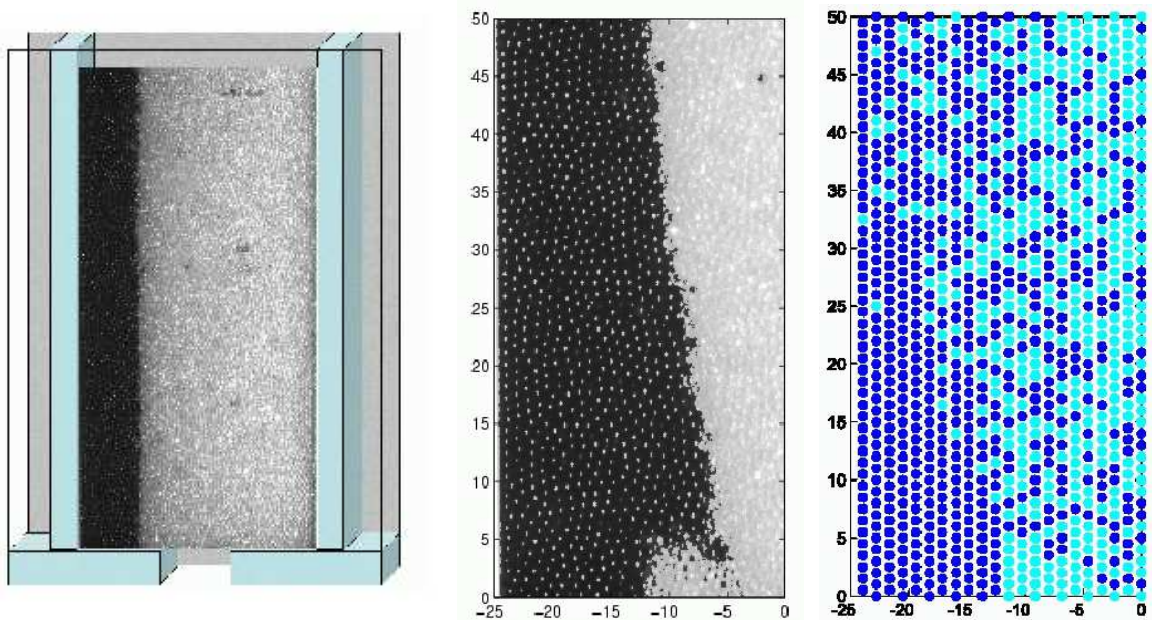


FIG. 5: Left: Experimental photograph of the initial condition of a quasi-two-dimensional silo with a vertical interface between black and white glass beads (by Jaehyuk Choi [37]). Center: The interface (in the left half of the silo) at a later time in the experiment. Right: A simulation of the same situation using the Void Model on a square lattice (by Guáqueta [98]). Length is measured in particle diameters ($d = 3\text{mm}$).

leave the silo at the same time. Thinking in terms of the Void Model, it could also mean that some extended entity causing motion is released into the bulk, once the orifice reaches a critical width.

This idea may seem strange, but it has a chance of being correct. The Void Model does reproduce one crucial feature of particle dynamics in slow, dense drainage experiments [37]: All fluctuations are independent of the flow rate, aside from a simple rescaling of time. One implication is that the Péclet number,

$$\text{Pe} = \frac{Ud}{D}, \quad (8)$$

is independent of the flow rate, or equivalently the diffusivity, D , is proportional to the local mean velocity, U . This strongly suggests that *diffusion and advection are caused by the same physical mechanism*, as in the Void Model. The common mechanism, however, cannot be the propagation of a void or a cage-breaking event, which implies $\text{Pe} \approx 1$. Instead, it seems to involve the cooperative motion of neighboring particles, which somehow results in much less diffusion, $\text{Pe} \gg 1$.

IV. THE SPOT HYPOTHESIS

A. A Mechanism for Cooperative Diffusion

In developing a microscopic theory, we are constrained by the fact that the mean velocity is fairly well described

by the Kinematic Model, which seems to imply the diffusion of some entity causing motion. Let us suppose that such an entity exists, but, since it cannot be a void, we will call it a “spot”. The kinematic parameter is then approximately set by the spot diffusion length,

$$b = \frac{\text{Var}(\Delta \mathbf{x}_s)}{2d_h \Delta z_s} \quad (9)$$

where $\Delta \mathbf{x}_s$ is the random horizontal displacement of a spot as it rises by Δz_s .

What exactly is a spot? Since spots are injected at the silo orifice as particles drain out, it is natural to assume that each carries a certain amount of free volume. Rather than being concentrated in a void, however, this volume should correspond to a *slight excess of interstitial space spread across an extended region*, typically larger than a particle, as shown in Fig. 6. We expect the size of a spot to be at least three particle diameters since it should induce the cooperative motion of a particle and its nearest neighbors.

The simplest dynamical hypothesis, illustrated in Fig. 7, is that *a spot causes all affected particles to move as a block* with the same small displacement in the opposite direction. As the spot follows its random trajectory upward, a thick chain of particles cooperatively reptates downward by a very small distance, much less than the particle diameter. The subsequent passage of other spots causes each particle to randomly reptate in many different thick chains, as shown in Fig. 6.

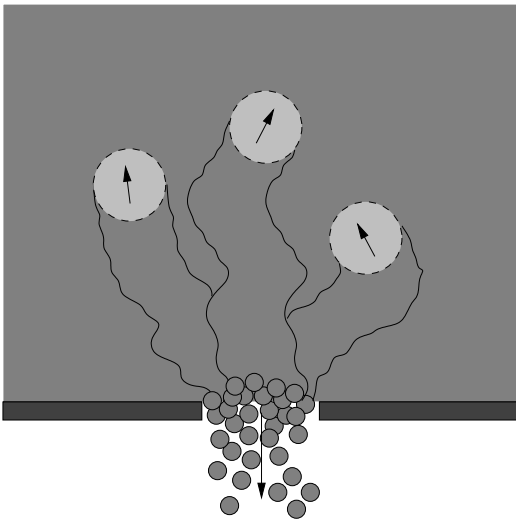


FIG. 6: The Spot Hypothesis I: Localized spots free interstitial volume, extending several particle diameters, diffuse upward from the silo orifice as particles drain out, causing the reverse reptation of thick chains of particles.

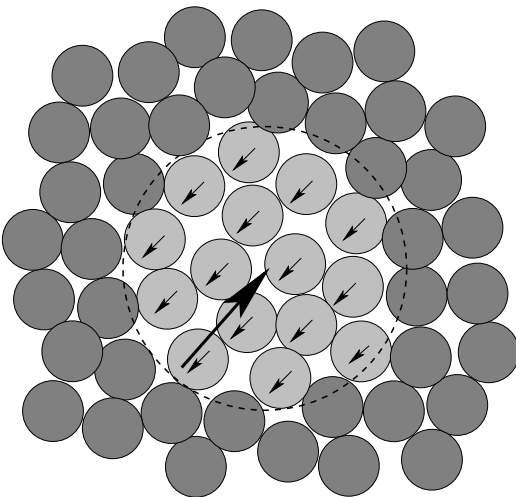


FIG. 7: The Spot Hypothesis II: Each spot displacement causes a block of neighboring particles to make a smaller displacement in the opposite direction, so as to roughly conserve the local volume.

Under this dynamics, the packing of particles is largely preserved because a pair of neighboring particles is usually affected by the same spot. Occasionally the pair finds itself near the edge of a spot, which causes a tiny relative displacement. The accumulated effect of such events gradually causes the particles to separate as they drain. The cage breaking length, however, is much larger than the particle size because relative displacements of neighbors are both small and rare. In fact, the cage-breaking length in the model (calculated below) can be comparable to the system size, as in experiments and simulations

of dense drainage.

This microscopic picture is fundamentally different from previous theories, which assume that particles undergo independent random walks. According to Kinetic Theory, a particle moves ballistically between instantaneous, randomizing collisions, and in the Void Model it jumps from cage to cage. In both cases, the particle loses a most of its neighbors in a single displacement, and thorough mixing occurs at the scale of several particle diameters.

B. Correlations Reduce Diffusion

A back-of-the-envelope calculation suffices to show that the spot hypothesis resolves the paradox of granular diffusion. Suppose that a spot carries a total free volume, V_s , and causes equal displacements, $(\Delta \mathbf{x}_p, \Delta z_p)$, among N_p particles of volume, V_p . The particle displacement can be related to the spot displacement, $(\Delta \mathbf{x}_s, \Delta z_s)$, by an approximate expression of total volume conservation,

$$N_s V_p (\Delta \mathbf{x}_p, \Delta z_p) = -V_s (\Delta \mathbf{x}_s, \Delta z_p), \quad (10)$$

which ignores boundary effects at the edge of the spot. From this relation, we can easily compute the particle diffusion length,

$$b_p = \frac{\text{Var}(\Delta \mathbf{x}_p)}{2d_h |\Delta z_p|} = \frac{w^2 \text{Var}(\Delta \mathbf{x}_s)}{2d_h w \Delta z_s} = w b \quad (11)$$

which is smaller than the spot (or volume) diffusion length by a factor,

$$w = \frac{V_s}{N_p V_p}, \quad (12)$$

equal to the ratio of the spot's free volume, V_s , to the total affected particle volume, $N_p V_p$. The Void Model corresponds to the unphysical limit where these volumes are both equal to a single particle volume ($N_p = 1, V_s = V_p, w = 1$), but generally we expect spots to affect multiple particles and carry relatively little excess volume ($N_p \gg 1, V_s < 1, w \ll 1$). The nontrivial implication of cooperative motion is then that particles diffuse much more slowly than volume, $b_p \ll b$, which resolves the paradox described above. Below we will show that the resolution is not just qualitative, but quantitative.

C. General Formulation of the Spot Model

The key mathematical concept in the Spot Model is that of a diffusing "region of influence", which causes correlated displacements among all particles within range. There are many possible microscopic postulates for this local cooperative motion, but the strong tendency to preserve nearly jammed packings suggests it should be

mainly a block translation as described above, plus perhaps a random block rotation, mostly involving nearest neighbors. For such rigid-body motions, however, the shear at the edge of a spot may be somewhat excessive.

More generally, we may allow the influence of a spot to be governed by a smooth function, $w(\mathbf{r}_p, \mathbf{r}_s)$, which decays quickly with distance from the spot center, $|\mathbf{r}_p - \mathbf{r}_s|$. For example, in the case of purely translational motion in one direction (opposing a spot displacement), the random displacement, $\Delta \mathbf{R}_p^{(i)}$, of the i th particle centered at $\mathbf{r}_p^{(i)}$, due to the random displacement, $\Delta \mathbf{R}_s^{(j)}$, of j th spot centered at $\mathbf{r}_s^{(j)}$ would be given by

$$\Delta \mathbf{R}_p^{(i)} = -w(\mathbf{r}_p^{(i)}, \mathbf{r}_s^{(j)} + \Delta \mathbf{R}_s^{(j)}) \Delta \mathbf{R}_s^{(j)} \quad (13)$$

We might expect a spot to roughly maintain its “shape” while moving through a system of particles, due to the local statistical regularity of random packings, so its influence function, w , should depend mainly upon the separation vector, $\mathbf{r}_p^{(i)} - \mathbf{r}_s^{(j)}$. This may change in regions of highly non-uniform flow, but in any case the spot influence should typically decay at separations, $|\mathbf{r}_p^{(i)} - \mathbf{r}_s^{(j)}|$, larger than a few particle diameters. Below we demonstrate that the mathematical model of Eq. (13) is a natural starting point for discrete simulations, as well as analysis in the continuum limit.

There are many possible extensions, which should be considered in future work. For example, the internal particle motion induced by a spot could contain a random component, or some other more complicated cooperative motion driven by inter-particle forces (see below). Different spots could also interact with each other by changing their drift velocity, diffusion length, size and/or free volume, which effectively induces cooperative particle motion at large scales. Weak repulsion and attraction might both occur, since the volume fraction tends to remain in a certain narrow range in a region of flow. Even if spots remain unchanged during motion, there could be statistical distributions of spot free volume, size, and shape, which might vary due to compaction and dilation processes driven by random spot annihilation, creation, and recombination. Such extensions may be necessary for a complete theory of dense granular flow, but in the next section we show that the basic model already compares well with silo-drainage experiments.

V. EXPERIMENTAL EVIDENCE

In this section, we consider the simplest version of the Spot Model, in which each spot carries the same free volume, V_s , and is spherical with a uniform influence, w , out to a distance R . We compare this model to experimental data, primarily from Ref. [37], including some new results by the same authors. The experiments provide compelling tests of the theoretical predictions, because the latter were made well in advance [100].

A. Free Volume and the Péclet Number

The Spot Model makes a quantitative connection between dilation, diffusion, and advection in a dense granular flow. As such, it predicts the Péclet number (8) in terms of typical local volume fluctuations. The Péclet number is independent of the flow rate, but, unlike with the Void Model, the predicted magnitude is consistent with experimental data.

We start with the general observation that the particle volume fraction, $\phi \approx 0.6$, varies by at most a few percent in the region of dense flow, away from the orifice. This is certainly a reasonable inference from drainage experiments, which maintain a nearly uniform density to the naked eye [37]. Detailed observations of particles near a glass silo wall confirm that the local area fraction varies by one to three percent at different flow rates [101]. Likewise, in granular dynamics simulations, the bulk volume fraction in thin horizontal cross sections varies in the range, $\phi \approx 0.565 - 0.605$, near the orifice, while staying within one or two percent of 0.60 in the region of steady dense flow far above the orifice [102].

These values are also consistent with studies of random packings of hard spheres in zero gravity. Rigidity percolation and dilatancy (expansion under shear stress) set in at $\phi \approx 0.55$ for “random loose packing” [103], which provides a rough lower bound on the volume fraction in a slow, dense flow. A rough upper bound is set by jammed random packing [11], e.g. in the “maximally random jammed state” ($\phi \approx 0.64$ [14] or $\phi \approx 0.63$ [15]) or the zero-temperature, zero-stress “jamming point” ($\phi \approx 0.63$ [16, 17]). Higher volume fractions also possible at the expense of some long-range crystalline order (e.g. as demonstrated by experiments with horizontal shaking [104]), up to the rigorous upper bound of $\phi = \pi/\sqrt{18} \approx 0.74$ for the FCC lattice [105], but such configurations are unlikely to permit quasi-steady flow.

If we attribute the maximum local reduction in volume fraction, $\Delta\phi/\phi \approx 0.01$, to the presence of N_s overlapping spots,

$$\Delta\phi = \phi - \frac{\phi}{1 + \phi w N_s} \approx \phi^2 w N_s, \quad (14)$$

then we have

$$w N_s \approx \frac{\Delta\phi}{\phi^2} \approx \frac{0.01}{0.6} \approx 0.02 \quad (15)$$

In that case, the Péclet number for horizontal diffusion would be

$$\text{Pe}_x = \frac{(|\Delta z_p|/\Delta t)d}{\text{Var}(\Delta \mathbf{x}_p)/2\Delta t} = \frac{d}{b_p} = \frac{d}{wb} \approx 40 N_s \quad (16)$$

for $b = 1.3d$. Since $N_s \geq 1$ in this calculation, we predict that a particle falls by on the order of 100 diameters before diffusing horizontally by one diameter.

This simple estimate is consistent with the experimental value, $\text{Pe}_x = 321$, for particles near a smooth wall in

slow drainage from a quasi-two dimensional silo [37]. It also suggests that spots occur at fairly high density, with as many as $N_s = 320/40 = 8$ overlapping in a position of high dilatancy. In a position of low dilatancy, where $\Delta\phi/\phi \approx 0.001$, it implies that spots typically do not overlap. Such a limited number of spot overlaps seems like a reasonable definition of a “dense” flow, where the simple picture in Eq. (7) could apply.

(Note that larger Péclet numbers in the range $Pe \approx 1500 - 3000$ have been reported for faster flows in long, narrow silos with shear-inducing rough walls [36]. In this case, the simple relation in Eq. (16) would imply a much higher spot density, where positions of 100 overlapping spots could be found. At such high spot densities (low volume fraction), it seems the model would no longer apply due to more independent particle displacements. Indeed, since Pe depends weakly on the flow rate, those experiments are not in the regime of slow drainage considered here. The data is also inconsistent with kinetic theories of dilute granular flow [36], so it seems to correspond to an intermediate regime of moderately dense flow.)

B. Spatial Velocity Correlations

The quantitative resolution of the granular-diffusion “paradox” provides some support for the Spot Model does not directly validate its microscopic hypothesis. How can we directly confirm or reject the existence of spots? The calculation above suggests that it would be impossible to observe the propagation of a single spot, but only large numbers of spots, which expectation is consistent with x-ray diffraction experiments showing fairly smooth density patterns in draining sand [106].

Rather than trying to observe a single spot, therefore, it makes more sense to seek statistical evidence of the passage of many spots. A direct signature of the cooperative motion in Fig. 7 is found in the spatial correlation function of velocity fluctuations (relative to a steady mean flow). Two particles are likely to fluctuate in the same direction when they are separated by less than a spot diameter because most spots engulf them at the same time. On the other hand, more distant particles are always affected by different spots, which implies independent fluctuations.

The spatial velocity correlation function, $C(r)$, for two particles separated by r is easily calculated for uniform, spherical spots of radius, R . The two instantaneous particle displacements are either identical (perfectly correlated), if they are caused by the same spot, or independent. Therefore, the correlation function, $C(r)$, is simply the scaled intersection volume, $\alpha(r; R)$, of two spheres of radius, R , separated by a distance, r :

$$\alpha(r; R) = 1 - \frac{3}{4} \frac{r}{R} + \frac{1}{16} \left(\frac{r}{R} \right)^2. \quad (17)$$

This result appears in a recent study of random point

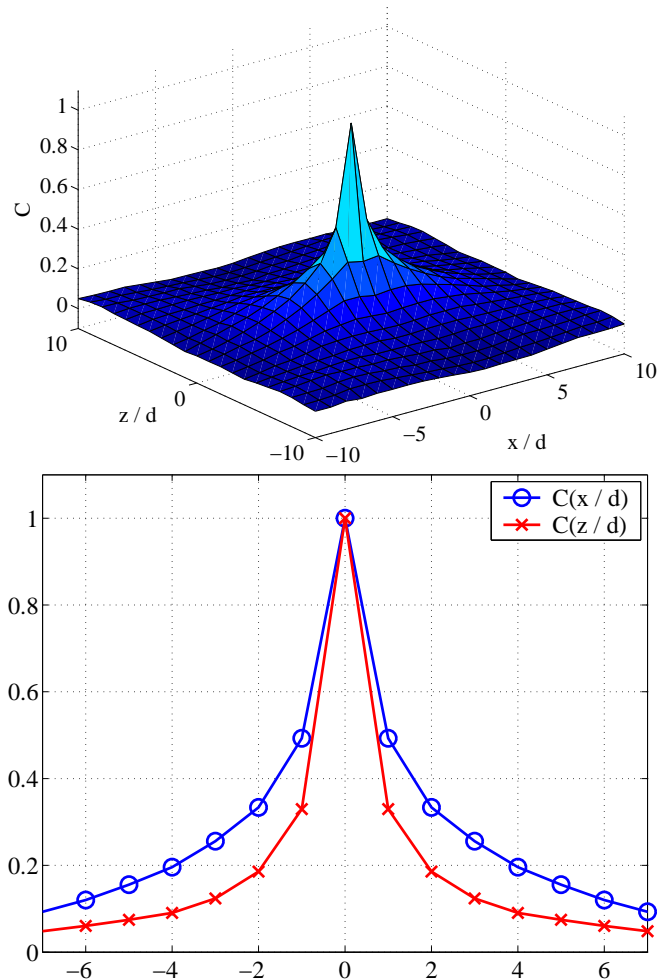


FIG. 8: Direct experimental evidence for spots: Spatial velocity correlations from the drainage experiments of Ref. [37]. Surface plot (top) and coordinate slices (bottom) of the correlation coefficient for velocity fluctuations (about the local mean flow) at horizontal separation, x , and vertical separation, z , in units of particle diameter, d . (Courtesy of Jaehyuk Choi.)

distributions [107], where $\alpha(r; R)$ is plotted in Fig. 9 (and earlier in Ref. [108]). The key point is that $C(r) = \alpha(r; R)$ decays to half its maximum value at a separation slightly smaller than spot radius, R . Similar curves result from other quickly decaying spot influence functions, such as exponentials or Gaussians (see below).

Motivated by this prediction, the experiments in Ref. [37] were performed to look for spatial velocity correlations in a real granular flow. Hundreds of glass beads ($d = 3\text{mm}$) near the wall of a quasi-two-dimensional draining silo were simultaneously tracked with 1ms resolution in time and $d/100$ in space in the region of non-uniform flow near the orifice. The data clearly reveals spatial velocity correlations, shown in Fig. 8, at the expected length scale of several particle diameters. It is

interesting that real spots are not quite spherically symmetric. The velocity correlations extend roughly twice as far in the horizontal direction as in the vertical direction, so these spots are more elliptical in shape. The data also implies a smooth decay of the spot influence function, $w(\mathbf{r}_p, \mathbf{r}_s)$, roughly an exponential decay. In contrast, for a uniform spot influence with a cutoff radius, R , the correlation function, $C(r) = \alpha(r, R)$, would decay roughly linearly to zero at $r = 2R$.

Leaving these interesting details for future analysis, we proceed with our assumption of uniform spot influence, as a good first approximation. As expected for cooperative motion largely preserving particle cages, the spot diameter is roughly five particle diameters, which corresponds to tens of affected particles per spot (say $N_p \approx 20$). Using Eq. (16) to infer spot influence,

$$w = \frac{d}{\text{Pe}_x b} = \frac{1}{(321)(1.3)} = 0.0024, \quad (18)$$

the simple relation, Eq. (12), then implies,

$$\frac{V_s}{V_p} = N_p w \approx 0.05 \quad (19)$$

In other words, *the interstitial free volume carried by a spot, although spread across tens of particles, is only a few percent of one particle volume.* Such small, coherent volume fluctuations are completely different from those postulated by the Void Model ($V_s = V_p$, $R = R_p$).

C. Cage Breaking

Further support for the spot hypothesis comes from experimental data on cage breaking [37], which also provides the most direct contradiction of the Void Model. Visual observation of particles in draining silos reveals that particle cages tend to persist for large distances, comparable to the system size. It is not unusual for some first neighbors to remain unchanged from the middle of the silo all the way to the orifice. A detailed analysis of the uniform-flow region far from the orifice yields a cage-breaking length, $z_c \approx 200d$, extrapolated from small falling distances, $\Delta z \leq 5d$. As such, the precise value, $200d$, should not be taken too seriously, but it is clear that cage breaking occurs very slowly in regions of low shear, at scales comparable to the system size. In contrast, the Void Model inevitably predicts cage-breaking at the scale of a single grain, $z_c \approx d$.

Rather than analyzing many-body cage dynamics in the Spot Model, it is simpler to consider two tracer particles, which are initially first neighbors, in a nearly uniform flow. Without correlations, the horizontal separation, X , would grow with distance dropped, z , like $X \approx d + \sqrt{2b_2 z}$, where the diffusion length for relative motion is twice that of single particles, $b_2 = 2b_p$, due to the additivity of variance. With correlations, the relative diffusion length,

$$b_2(X) = 2b_p [1 - C(X)], \quad (20)$$

is reduced by a factor, $1 - C(X) \approx d/2R$ (for $X \approx d$). Supposing that cage breaking occurs at $X \approx 2d$, we predict a cage-breaking length, $z_c = d^2/2b_2$, of roughly,

$$\frac{z_c}{d} \approx \frac{R}{2b_p} = \frac{\text{Pe}_x R}{2d} \approx \text{Pe}_x \quad (21)$$

where we take the approximation, $R \approx 2d$, from the data in Fig. 8. The relation, $z_c \approx \text{Pe}_x d \approx 300d$, is quite consistent with the experimental data.

D. Vertical Diffusion

We have postulated that spots diffuse upward with a horizontal diffusion length equal to the kinetic parameter, $b_s^\perp = b$, because the mean velocity roughly follows the profile of the Kinematic Model, as shown in Fig. 1. By looking at fluctuations, we can also infer the vertical diffusion length of spots, which would be difficult to measure directly in experiments. (Note that voids exhibit zero vertical diffusion, unless one introduces a random waiting time between steps.)

Suppose that the vertical component of the spot displacement, Δz_s , is a positive random variable with a finite mean, $\langle \Delta z_s \rangle$. We can then define the vertical diffusion length of spot,

$$b_s^\parallel = \frac{\text{Var}(\Delta z_s)}{2d_h \langle \Delta z_s \rangle}, \quad (22)$$

by analogy with Eq. (9) for the horizontal diffusion length (where Δz_s should be replaced by $\langle \Delta z_s \rangle$). In a similar way, we define the vertical diffusion length of particles, b_p^\parallel (and $b_p^\perp = b_p$).

Assuming that the spot influence does not distinguish between different velocity components, as in Eq. (10), we have the identity,

$$w = \frac{b_p^\parallel}{b_s^\parallel} = \frac{b_p^\perp}{b_s^\perp}. \quad (23)$$

This allows us to infer the vertical diffusion length of spots from that of particles,

$$b_s^\parallel = \frac{b_p^\parallel}{w} = \frac{d}{\text{Pe}_z w} = \frac{d}{(150)(0.0024)} = 2.8d \quad (24)$$

where we take $\text{Pe}_z = 150$ from experiments [37]. This calculation assumes that the dominant contribution to the particle vertical diffusivity is the influence of the spot vertical diffusivity, and not the random arrival of different spots (consistent with the mean-field analysis of section VII). Since $b_s^\parallel/b_s^\perp = 2.8/1.3 \approx 2$, the spot displacements in these experiments fluctuate twice as much in the vertical direction as in the horizontal direction.

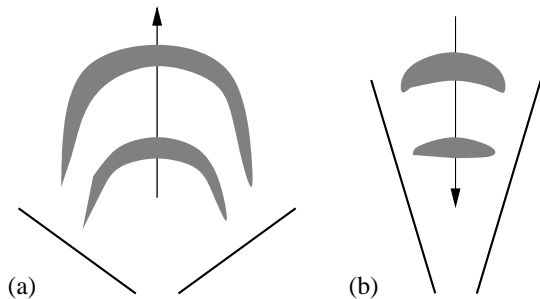


FIG. 9: Sketch of nonlinear waves of free volume (gray regions) observed in funnels of draining sand [106]. For the same orifice width, the waves propagate upward for large opening angles (a) and sometimes downward for small opening angles (b).

E. Spot Interactions and Density Waves

Until now, we have assumed that spots undergo independent random walks. This suffices to describe many aspects of silo drainage, so we conclude that spot interactions are relatively weak in such flows. Nevertheless, there must be short-range interactions between spots to keep the local volume fraction in the typical range for dense, gravity-driven flows ($0.56 \leq \phi \leq 0.61$). Physically, spot repulsion should derive from the tendency for particles to quickly collapse from all directions toward a region of overly low volume fraction ($\phi < 0.56$). Because each spot carries very little volume, the repulsion should only become strong when many spots overlap (e.g. $N_s > 10$). Similarly, spot attraction follows from the tendency of free volume to avoid nearly jammed regions ($\phi > 0.61$) if it can be accommodated in an already flowing region. This attraction should strengthen as spots become more dilute ($N_s \leq 1$), e.g. sharpening the boundary between flowing and stagnant regions in Fig. 1.

Is there any evidence for spot interactions in experiments? An indirect sign could be the density waves observed by Baxter *et al.* in three-dimensional draining funnels of rough sand using x-ray diffraction [106]. The authors gave a heuristic explanation of such waves in terms of the formation and collapse of arches across the central region but did not attempt a quantitative theory. As sketched in Fig. 9, the observed density patterns were mostly consistent with upward moving waves of reduced density, but downward moving waves were also inferred in some narrow funnels. Nonlinear wave equations for dilute flows [109] have been derived from the kinetic theory of inelastic gases [28], but there does not appear to be a microscopic theory for density waves in dense flows.

Subsequent authors [110, 111, 112] have suggested an analogy with nonlinear kinematic waves in traffic flow [113], and some have even claimed that granular flow and traffic flow are in the same “universality class” [114]. The classical, continuum theory of traffic waves describes the effective short-range repulsion between cars trying to

avoid an accident by a flux-density relation, $q(\rho)$, with a maximum at ρ_c . The conservation law for the car density,

$$\frac{\partial \rho}{\partial t} + \frac{\partial q}{\partial z} = \frac{\partial \rho}{\partial t} + c(\rho) \frac{\partial \rho}{\partial x} = 0, \quad (25)$$

then involves the characteristic velocity, $c(\rho) = q'(\rho)$, which changes sign at ρ_c , implying that density waves propagate forward in light traffic ($\rho < \rho_c$) and backward in heavy traffic ($\rho > \rho_c$). Whenever density variations are generated (by noise, boundary conditions, etc.), they combine into coherent structures terminated on one side by a shock and on the other by an expansion fan.

Granular shock waves in two-dimensional inclined funnels and pipes have been studied extensively in simulations [111, 112, 115] and particle-tracking experiments [62, 63]. A detailed study of shock statistics [63] has revealed differences with simple traffic-flow models, although somewhat similar average $q(\rho)$ curves have been measured. Granular dynamics simulations also show that friction among the particles and walls initiates the fluctuations leading to shock formation [110].

The Spot Model provides a simple microscopic explanation for the experimental observations. Given our expectation of weak spot repulsion, it is natural to think of spots as “cars” moving upward in a dense flow. For a given orifice width, a funnel with a large opening angle, as in Fig. 9(a), should have a fairly low spot density as a result of lateral diffusion. In that case ($\rho_s < \rho_c$), nonlinear spot waves initiated by fluctuations at the orifice propagate upward at nearly the spot drift velocity, slowly organizing into coherent structures of reduced density. The backside of the wave forms shock, below which the particle density suddenly increases. Particles gradually accelerate into the looser spot-rich region and suddenly slow down upon entering the more compact region below.

As the funnel angle is reduced (for the same orifice width), spots are increasingly reflected by the boundaries into the central region, where their density goes up. The crowding of spots could eventually cause a reversal of density waves, analogous to the familiar backward-moving waves of heavy traffic. In that case ($\rho_s > \rho_c$), a region of reduced spot density would form a shock on its back (upper) side, which the particles would see as downward moving compaction wave. On the other hand, a region of increased spot density would form a shock on its front (lower) side, corresponding to a downward moving rupture zone.

It would be interesting to revisit experimental density patterns in light of the Spot Model. Density waves in wide funnels ($\rho_s < \rho_c$) should move as weakly interacting “tracer spots”, thus revealing the spatial profile of spot drift and diffusivity. For example, the wave patterns sketched in Fig. 9(a) suggest that the spot drift velocity and diffusion length are smaller near the stagnant region than in the faster-flowing central region.

F. Crossover from Super to Normal Diffusion

We have already mentioned the surprising result of particle tracking in draining silos that all fluctuations depend on the distance dropped, not time, over a wide range of flow rates [37]. For the mean-squared displacement relative to the mean flow, there is a universal crossover from super-diffusion to normal diffusion after a particle falls by roughly one diameter. The observed super-diffusive regime, $0.005d < |\Delta x| < 0.5d$, is not ballistic ($|\Delta x| \propto t \propto z$) but instead exhibits a non-trivial scaling exponent, $\Delta x \propto t^{0.75} \propto z^{0.75}$.

A small-scale ballistic regime has also been inferred by diffusing wave spectroscopy for glass beads ($d = 95\mu\text{m}$, $v = 0.32\text{ cm/s}$) flowing down a vertical pipe toward a wire mesh [116]. The data does not seem of indicative of thermal collisions, however, since the “collision distance”, $l_c = 28\text{ nm} \approx 10^{-5}d$, is surely at the scale of surface roughness. Moreover, the “collision time”, $\tau_c = 9\mu\text{s} \approx 10^{-4}d/v$, implies a typical velocity, $l_c/\tau_c = 0.31\text{ cm/s}$, equal to the mean flow speed, which seems hard to attribute to independent thermal fluctuations. In any case, no transition to diffusion is observed at this scale, so these nano-collisions are not of the randomizing type postulated by kinetic theory and have little bearing on our discussion of structural rearrangements.

Returning to the particle-tracking data, we have seen that the Spot Model describes the diffusive regime with quantitative accuracy, but the super-diffusive regime is not so easily explained. Spots are not constrained to move on a lattice, so the size of the spot displacements is arbitrary, as long as the horizontal spot diffusion length equals the kinetic parameter, $b_s^\perp = b \approx d$. For example, each spot could follow a persistent random walk in which successive, small random displacements ($\Delta z_s \ll d$) have a correlation coefficient, γ . Following Taylor [91, 93], the kinetic parameter would then be

$$\frac{b}{b_0} = \frac{1 + \gamma}{1 - \gamma} \quad (26)$$

where b_0 is the spot diffusion length in the absence of auto-correlations, given by Eq. (9). For $0 < \gamma < 1$, the persistent random walk of the spot has ballistic scaling up to a crossover distance, $-\Delta z_s / \log \gamma$, which should be of order d , since $b \approx d$. Since the spot diameter is larger than d , a single particle is affected many times by the same spot, so the particle would inherit a persistent random walk with ballistic motion up to a crossover distance of roughly $w d \ll d$.

This scaling and crossover distance do not agree with experiment, but various modifications could perhaps resolve the discrepancy. It is straightforward to achieve sub-ballistic scaling with longer-range, power-law auto-correlations between spot steps, although some cutoff would be needed to preserve the normal diffusive regime. More likely, however, the super-diffusive regime is associated with more complicated particle motion caused by

spots. The simple picture in Fig. 7 ignores packing constraints and frictional contacts, so we should expect additional microscopic rearrangements to occur, superimposed on the mean spot-induced motion. This fundamental issue becomes more clear in simulations of the model.

VI. SPOT-BASED SIMULATIONS

A. Statistical Dynamics of Dense Flow

The Spot Model provides a very simple and efficient Monte Carlo algorithm for dense granular drainage. The simulation begins with a given distribution of tracer particles, either on a lattice or in a random packing. The particles then move passively in response to spots undergoing directed random walks upward. Spots are injected randomly in time and space along the orifice to artificially set the flow rate. (Our theory makes no prediction about how spots are created, which is related to the poorly understood connection between flow rate and orifice width.)

For illustration purposes, we consider the simplest version of the model in two dimensions without boundaries. Let us assume that spots undergo independent, directed random walks upward on a lattice (without interactions). The vertical spot lattice parameter is set on the order of a particle diameter, d , and the horizontal lattice parameter is constrained by kinetic parameter, b , via Eq. (9). Alternatively, for smoother spot motion using a persistent random walk, the vertical lattice parameter may be reduced for a desired level of auto-correlation, say $\gamma = 0.5$, where b is now set by Eq. (26). We further assume Eq. (10) for the spot influence, where each particle within a distance, R , from the spot center (after a displacement), receives the same anti-parallel displacement, smaller by a factor, w .

Spot simulations of the experiments in Fig. 1 and 5 are shown in Fig. 10 and 11, respectively. The spot parameters determined from independent experimental measurements, as described above ($b = 1.3d$, $R = 2.5d$, $w = 0.0024$), without any *ad hoc* fitting. The result is a dramatic improvement over the simulations in Figs. 4 and 5(c) of the same situations using the Void Model, which produces far more mixing. Remarkably, the mean flow profile is nearly the same in all cases, given by Eq. (3), even though the particle dynamics is radically different.

It is visually apparent that the Spot Model resolves the “paradox of granular diffusion”. Detailed analysis (to appear elsewhere) shows that the experimental dynamics of two-color interfaces is reproduced rather well by simulations, as in Fig. 11. The interface remains sharp while moving with the mean flow and slowly developing fluctuations at the scale of the spot size.

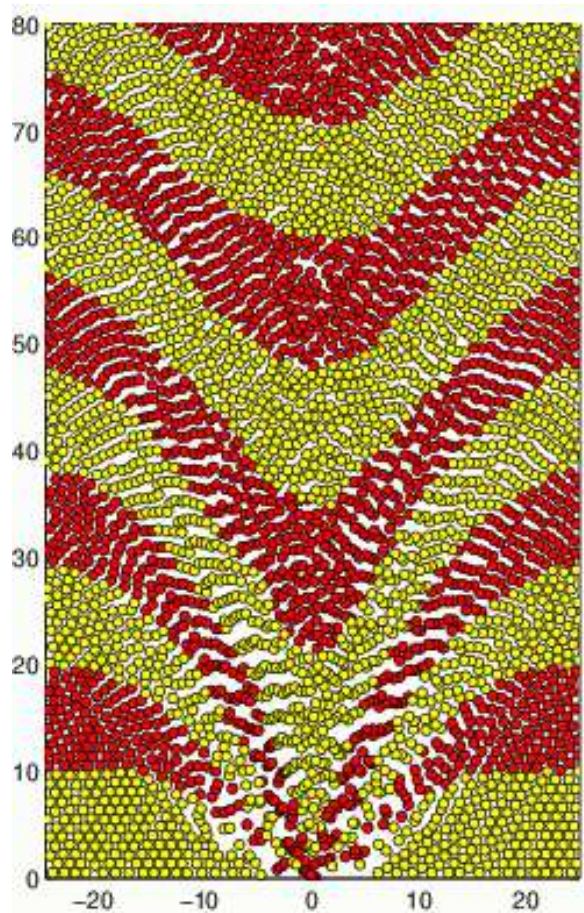


FIG. 10: A spot simulation of the experiment in Fig. 1, to be compared with the void simulation in Fig. 4. (Courtesy of Jaehyuk Choi.)

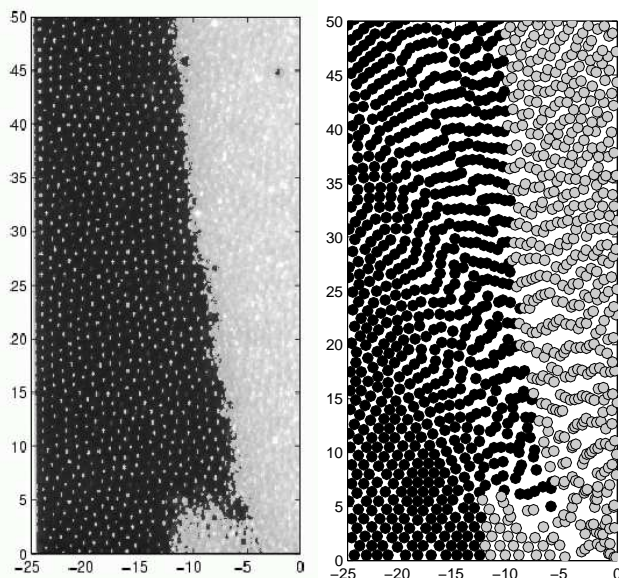


FIG. 11: A spot-model simulation (right) of the experiment in Fig. 5 (left).

B. Density Fluctuations and Packing Constraints

The reader may have noticed something strange about the simulations in Figs. 10 and 11 — the nearly uniform density of particles is not preserved. In regions of shear, the particles form dense overlapping bands separated by thin vacuum bands transverse to the shear direction. Although mesoscopic shear bands do form in disordered materials, such as metallic glasses (see section IX), these bands are at the particle scale, and hence are not physical. At the lower edges of the flow region, where the shear rate is highest, the fluctuations intensify, while directly above the orifice the density increases.

We conclude that the simplest version of the Spot Model does not completely describe the joint probability distribution of all particles, even though it predicts the marginal distribution of each tracer particle quite well. As expected, what is missing is a strict enforcement of packing constraints. The block-like cooperative motion in spots causes density fluctuations to grow very slowly, but unphysical structures eventually arise.

Stabilizing the density with a simple analytical modification is likely to be difficult. As discussed above, density-preserving extra fluctuations appear to be related to the super-diffusive regime seen in experiments, which has a nontrivial, sub-ballistic scaling. Moreover, we should not expect to be able to generate a multitude of random close packings by a simple statistical model. Even without flow, the sampling of random close packings is a challenging computational problem in its own right, which seems to require brute-force molecular dynamics [12, 14, 15, 16, 17, 18].

On the other hand, unphysical density fluctuations also arise in the standard kinetic theory of liquids, when particles undergo independent random walks. In dilute gases, this assumption correctly predicts Poisson-distributed density fluctuations, where the variance in the particle number scales with the volume [117], but in a liquid, just as in a granular material, this picture is incorrect. Packing constraints during flow somehow preserve much smaller, “hyper-uniform” density fluctuations, where the variance scales with the surface area, as in the case of a regular lattice [107]. It is fair to say that a collective statistical theory of liquids, molecular or granular, has not yet been developed, so we should not be easily deterred.

C. Multiscale Algorithms for Dense Flows

We have seen that the collective particle dynamics in the Spot Model is quite realistic, aside from slowly growing density fluctuations, so it may be that only occasional small perturbations could suffice to preserve the density. For example, after some (or all) spot-induced cooperative displacements, the affected particles could be relaxed to equilibrium with simple spring-like forces, perhaps including the effect of gravity. The center of mass of the block of displaced particles should be constrained during

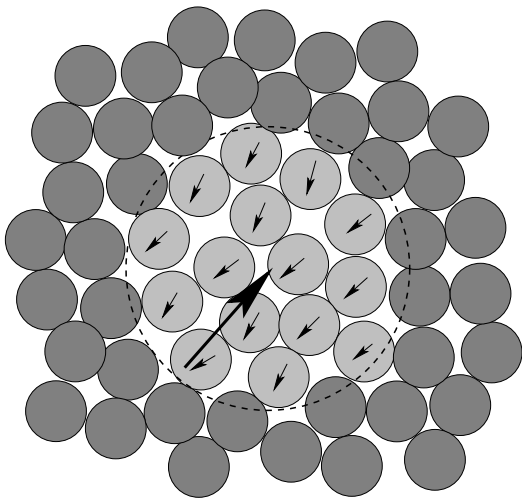


FIG. 12: The Spot Hypothesis III: Real spots also cause small internal rearrangements driven by packing constraints (relative to the average motion shown in Fig. 7). In a multiscale simulation algorithm, this could be done by a constrained relaxation following the mean spot-induced displacements.

relaxation to prevent slipping back into the initial positions. A preliminary implementation of this idea using a soft-core repulsion between grains (without gravity or friction) produces rather realistic bulk flows with a stable density [118].

Regardless of the detailed implementation, fixing the density will result in some additional cooperative fluctuations relative to the mean spot-induced displacement, as shown in Fig. 12. This is surely a more realistic picture of a dense flow, which incorporates the microscopic inter-particle forces into a new kind of multiscale simulation algorithm. In spite of the potentially expensive relaxation step, such an algorithm is much more efficient than brute-force molecular dynamics tracking all particle contacts. It takes advantage of spots to accelerate the dynamics, while keeping the system in a nearly jammed state.

This would be an interesting direction to pursue, not only for simulations, but also to gain insight into the basic physics of dense flows. Unlike the mean spot-induced motion, the extra fluctuations to preserve the density are correlated over the passage of multiple spots. The result could be a crossover from super to normal diffusion after a particle interacts with many spots, perhaps once it falls by its own diameter. Understanding such small-scale fluctuations is a fundamental open question.

VII. THE CONTINUUM LIMIT

Macroscopic approximations offer many advantages over microscopic theories, whenever a clear connection can be made. Both analytical and numerical solutions are usually much easier starting from a continuum ap-

proximation than an underlying discrete model. Moreover, various poorly understood microscopic details are swept into parameters in the continuum equations, which (one hopes) capture the essential physics in a robust way. A good example is the simultaneous description of Brownian motion, financial time series, and heat transfer by the diffusion equation. Perhaps even more remarkable is continuum hydrodynamics, which hides our ignorance of collective statistical dynamics in liquids. In this section, we derive continuum equations for diffusion and flow in the Spot Model based on the simple picture of Fig. 7, thus ignoring the complicated density-preserving relaxation in Fig. 12.

A. A Nonlocal Stochastic Differential Equation

We begin by partitioning space as shown Fig. 13, where the n th volume element, $\Delta V_s^{(n)}$, centered at $\mathbf{r}_s^{(n)}$ contains a random number, $\Delta N_s^{(n)}$, of spots at time t (typically one or zero). In a time interval, Δt , suppose that the j th spot in the n th volume element makes a random displacement, $\Delta \mathbf{R}_s^{(j)}(\mathbf{r}_s^{(n)})$ (which could be zero). According to Eq. (13), the total displacement, $\Delta \mathbf{R}_p$, of a particle at \mathbf{r}_p in time Δt is then given by a sum of all the displacements induced by nearby spots,

$$\Delta \mathbf{R}_p(\mathbf{r}_p) = - \sum_n \sum_{j=1}^{\Delta N_s^{(n)}} w(\mathbf{r}_p, \mathbf{r}_s^{(n)} + \Delta \mathbf{R}_s^{(j)}(\mathbf{r}_s^{(n)})) \Delta \mathbf{R}_j^{(n)}(\mathbf{r}_s^{(n)}) \quad (27)$$

Note that the spatio-temporal distribution of spots, $\Delta N_s^{(n)}$, is another source of randomness, in addition to the individual spot displacements, $\Delta \mathbf{R}_j^{(n)}$, so that each particle displacement is given by a random sum of random variables.

In the continuum limit, we arrive at a non-local, non-linear stochastic differential equation (SDE):

$$d\mathbf{R}_p(\mathbf{r}_p, t) = - \int dN_s(\mathbf{r}_s, t) w(\mathbf{r}_p, \mathbf{r}_s + d\mathbf{R}_s(\mathbf{r}_s, t)) d\mathbf{R}_s(\mathbf{r}_s, t), \quad (28)$$

where the stochastic integral is defined by the limit of the random Riemann sum in Eq. (27). This equation differs from standard nonlinear SDEs in two basic ways: (i) The tracer trajectory,

$$\mathbf{r}_p(t) = \int_{\tau=0}^t d\mathbf{R}_p(\mathbf{r}_p, \tau) \quad (29)$$

is passively driven by a stochastic distribution of moving influences (spots), $dN_s(\mathbf{r}_s, t)$, which evolves in time and space, rather than by some internal source of independent fluctuations, and (ii) the stochastic differential, $d\mathbf{R}_p(\mathbf{r}_p, t)$, is given by a non-local integral over other stochastic differentials, $d\mathbf{R}_s(\mathbf{r}_s, t)$, associated with these moving influences, which lie at finite distances away from the particle.

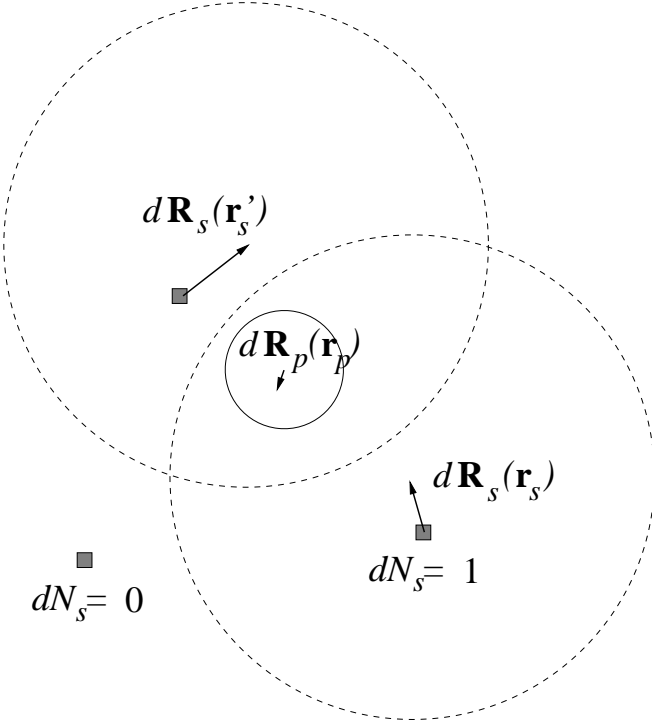


FIG. 13: Sketch of a particle interacting with a collection of passing spots, showing some of the quantities involved in defining the nonlocal SDE, Eq. (28).

B. Mean-field Fokker-Planck Equation

Equation (28) seems to be a new type of SDE, for which a mathematical theory needs to be developed. Here, we begin deriving analytical results based on the assumption that all the stochastic differentials for particle displacements in Eq. (29) are independent. This ignores the fact that the spot distribution at one time, $dN_s(\mathbf{r}_s, t)$, depends explicitly on the distribution and displacements at the previous time, $t - dt$. Even for a stationary spot distribution, it also ignores the fact that each spot, due to its extended influence, generally affects the same particle more than once, so that any autocorrelations in spot motion are partly transferred to the particles.

Assuming independent displacements, the propagator, $P_p(\mathbf{r}, t | \mathbf{r}_0, t_0)$, which gives the probability density of finding the particle at \mathbf{r} at time t after being at \mathbf{r}_0 at time t_0 , satisfies a Fokker-Planck (or forward Kolmogorov) equation [119],

$$\frac{\partial P_p}{\partial t} + \nabla \cdot (\mathbf{u}_p P_p) = \nabla \nabla : (\mathbf{D}_p P_p), \quad (30)$$

with drift velocity,

$$\mathbf{u}_p(\mathbf{r}, t) = \frac{\langle d\mathbf{R}_p(\mathbf{r}, t) \rangle}{dt} = \lim_{\Delta t \rightarrow 0} \frac{\langle \Delta \mathbf{R}_p(\mathbf{r}, t) \rangle}{\Delta t}, \quad (31)$$

and diffusivity tensor,

$$\mathbf{D}_p^{\alpha\beta}(\mathbf{r}, t) = \frac{\langle dR_p^\alpha dR_p^\beta \rangle}{2 dt}. \quad (32)$$

(Here $\nabla \nabla : \mathbf{A}$ denotes $\sum_\alpha \sum_\beta \frac{\partial^2 A^{\alpha\beta}}{\partial x_\alpha \partial x_\beta}$.) The Fokker-Planck coefficients may be calculated by taking the appropriate expectations using Eq. (27) in the limits $\Delta V_s^{(n)} \rightarrow 0$ and then $\Delta t \rightarrow 0$, which is straightforward if we assume (as above) that spots do not interact. In this approximation, the spot displacements, $\Delta \mathbf{R}_s^{(j)}(\mathbf{r}_s^{(n)})$, and the local numbers of spots, $\Delta N_s^{(n)}$, are independent random variables within each infinitesimal time interval. They are also independent of the same variables at earlier times, as assumed above.

In order to calculate the drift velocity, we need only the mean spot density, $\rho_s(\mathbf{r}_s, t)$, defined by $\langle \Delta N_s^{(n)} \rangle = \rho_s(\mathbf{r}_s, t) \Delta V_s^{(n)}$. The result,

$$\mathbf{u}_p(\mathbf{r}_p, t) = - \int dV_s w(\mathbf{r}_p, \mathbf{r}_s) [\rho_s(\mathbf{r}_s, t) \mathbf{u}_s(\mathbf{r}_s, t) - 2 \mathbf{D}_s(\mathbf{r}_s, t) \cdot \nabla \rho_s(\mathbf{r}_s, t)] \quad (33)$$

exhibits two sources of drift. The first term in the integrand simply opposes the spot drift velocity,

$$\mathbf{u}_s(\mathbf{r}, t) = \frac{\langle d\mathbf{R}_s(\mathbf{r}, t) \rangle}{dt}, \quad (34)$$

as in the heuristic equation (10). The second term, which depends on the spot diffusion tensor,

$$\mathbf{D}_s^{(i,j)}(\mathbf{r}, t) = \frac{\langle dR_s^{(i)} dR_s^{(j)} \rangle}{2 dt}, \quad (35)$$

is a “noise-induced drift” (typical of nonlinear SDEs [119]) causing particles to climb gradients in the spot density. Both effects are averaged over nearby regions, weighted by the spot influence function, $w(\mathbf{r}_p, \mathbf{r}_s)$.

In order to calculate the diffusivity tensor, we also need information about fluctuations in the spot density. Continuing with our “mean-field approximation”, it is natural to assume independent spot fluctuations,

$$\langle \Delta N_s^{(n)} \Delta N_s^{(m)} \rangle = \delta_{m,n} \langle (\Delta N_s^{(n)})^2 \rangle = O((\Delta V_s^{(n)})^\nu), \quad (36)$$

where $\nu = 1$ for a Poisson process and $\nu < 1$ for a hyperuniform process [107]. It turns out that such fluctuations do not contribute to the diffusion tensor (in more than one dimension), and the result is

$$\mathbf{D}_p(\mathbf{r}_p, t) = \int dV_s w(\mathbf{r}_p, \mathbf{r}_s)^2 \rho_s(\mathbf{r}_s, t) \mathbf{D}_s(\mathbf{r}_s, t). \quad (37)$$

Note that the influence function, w , appears squared in Eq. (37) and linearly in Eq. (33). This causes the Péclet number for tracer particles to be of order $1/w$ smaller

than that of spots (or free volume), as was derived heuristically above in Eq. (11).

An interesting general observation about Equation (30) with coefficients (33) and (37) is that rescaling the spot density is equivalent to rescaling time. In other words, all aspects of the stochastic motion of a tracer particle, including its Péclet number, are determined by geometry, independent of the total flow rate (or average spot density). As explained above, this experimental observation is in qualitative disagreement with kinetic theory and quantitative disagreement with the Void Model. On the other hand, the fact that fluctuations are proportional to the spot density suggests that a meaningful definition of “temperature” for dense granular flows (if one exists) might simply depend on the free volume of random packings. This possibility is discussed below in section IX.

Higher-order terms a Kramers-Moyall expansion generalizing Eq. (30) for finite independent displacements, which depend on fluctuations in the spot density, are straightforward to calculate, but beyond the scope of this paper. Such terms are typically ignored in stochastic analyses because, in spite of improving the overall approximation, they tend to produce small negative probabilities in the tails of distributions [119]. For dense granular flows described by Eq. (28), however, they may be important since displacements can be relatively large compared to spatial variations in probability density. This is the case in highly nonuniform flows, such as near the orifice of a silo, where mean velocities may vary on the scale of a few particle diameters.

C. Spatial Velocity Correlation Tensor

For any stochastic process representing the motion of a single particle, it is well-known that transport coefficients can be expressed in terms of *temporal* correlation functions via the Green-Kubo relations [119]. For example, the diffusivity tensor in a uniform flow is given by the time integral of the velocity auto-correlation tensor,

$$D_p^{\alpha\beta} = \int_0^\infty dt \langle U_p^\alpha(t) U_p^\beta(0) \rangle \quad (38)$$

where $\mathbf{U}_p(t) = \{\mathbf{U}_p^\alpha\} = d\mathbf{R}_p/dt$ is the stochastic velocity of a particle. (A similar relation holds for spots.)

In the Spot Model, nearby particles move cooperatively, so the transport properties of the collective system also depend on the two-point *spatial* velocity correlation tensor,

$$C_p^{\alpha\beta}(\mathbf{r}_1, \mathbf{r}_2) = \frac{\langle U_p^\alpha(\mathbf{r}_1) U_p^\beta(\mathbf{r}_2) \rangle}{\sqrt{\langle U_p^\alpha(\mathbf{r}_1)^2 \rangle \langle U_p^\beta(\mathbf{r}_2)^2 \rangle}} \quad (39)$$

which is normalized so that $C_p^{\alpha\beta}(\mathbf{r}, \mathbf{r}) = 1$. We emphasize that the expectation above is conditional on finding two particles at \mathbf{r}_1 and \mathbf{r}_2 at a given moment in time and

includes averaging over all possible spot distributions and displacements. Substituting the SDE (28) into Eq. (39) yields

$$C_p^{\alpha\beta}(\mathbf{r}_1, \mathbf{r}_2) = \frac{\int dV_s \rho_s(\mathbf{r}_s) D_s^{\alpha\beta}(\mathbf{r}_s) w(\mathbf{r}_1, \mathbf{r}_s) w(\mathbf{r}_2, \mathbf{r}_s)}{\sqrt{D_p^{\alpha\beta}(\mathbf{r}_1) D_p^{\alpha\beta}(\mathbf{r}_2)}} \quad (40)$$

where we have assumed again that spots do not interact (independent displacements).

Equation (40) is a new kind of integral relation for cooperative diffusion, which relates the spatial velocity correlation tensor to the spot (or free volume) diffusivity tensor via integrals of the spot influence function, $w(\mathbf{r}_p, \mathbf{r}_s)$. If the statistical dynamics of spots is homogeneous (in particular, if \mathbf{D}_s is constant), then the relation simplifies:

$$C_p^{\alpha\beta}(\mathbf{r}_1, \mathbf{r}_2) = \frac{\int dV_s \rho_s(\mathbf{r}_s) w(\mathbf{r}_1, \mathbf{r}_s) w(\mathbf{r}_2, \mathbf{r}_s)}{\sqrt{\int dV_s \rho_s(\mathbf{r}_s) w(\mathbf{r}_1, \mathbf{r}_s)^2 \int dV'_s \rho_s(\mathbf{r}'_s) w(\mathbf{r}_2, \mathbf{r}'_s)^2}} \quad (41)$$

if $D_s^{\alpha\beta} \neq 0$ (and 0 otherwise). If the statistical dynamics of particles is also homogeneous, as in a uniform flow ($\rho_s = \text{constant}$), then it simplifies even further:

$$C_p^{\alpha\beta}(\mathbf{r}) = \frac{\int dV_s w(\mathbf{r} - \mathbf{r}_s) w(-\mathbf{r}_s)}{\int dV_s w(\mathbf{r}_s)^2} \quad (42)$$

where we have assumed that the spot influence function, and thus the correlation tensor, are translationally invariant ($\mathbf{r} = \mathbf{r}_1 - \mathbf{r}_2$). These predictions may be used to infer the spot influence function experimental measurements, as in Eq. (17) above for uniform spots with sharp cutoff. For the case of a symmetric Gaussian spot of width σ in each direction,

$$w(\mathbf{r}) = \frac{V_s}{(2\pi\sigma^2)^{3/2}} e^{-r^2/2\sigma^2}, \quad (43)$$

an even simpler formula results from the overlap integral,

$$C_p^{\alpha\beta}(\mathbf{r}) = e^{-r^2/4\sigma^2}. \quad (44)$$

D. Relative Diffusion of Two Tracers

The spatial velocity correlation function affects many-body transport properties. For example, the relative displacement of two tracer particles, $\mathbf{r} = \mathbf{r}_1 - \mathbf{r}_2$, has an associated diffusivity tensor given by,

$$D^{\alpha\beta}(\mathbf{r}_1, \mathbf{r}_2) = D_p^{\alpha\beta}(\mathbf{r}_1) + D_p^{\alpha\beta}(\mathbf{r}_2) - 2 C_p^{\alpha\beta}(\mathbf{r}_1, \mathbf{r}_2) \sqrt{D_p^{\alpha\alpha}(\mathbf{r}_1) D_p^{\beta\beta}(\mathbf{r}_2)} \quad (45)$$

In a uniform flow, the diagonal components take the simple form

$$D^{\alpha\alpha}(\mathbf{r}) = 2 D_p^{\alpha\alpha} (1 - C_p^{\alpha\alpha}(\mathbf{r})) \quad (46)$$

which was used above to estimate the cage-breaking length. A more detailed calculation of the relative propagator, $P(\mathbf{r}, t | \mathbf{r}_0, t_0)$, neglecting temporal correlations (as above) would start from the associated Fokker-Planck equation,

$$\frac{\partial P(\mathbf{r}, t)}{\partial t} = \nabla \nabla : (\mathbf{D}(\mathbf{r}) P(\mathbf{r}, t)) \quad (47)$$

with a delta-function initial condition. (In a non-uniform flow, one must also account for spurious drift and motion of the center of mass.)

Our simplified analysis does not enforce packing constraints, so it allows for two particles to be separated by less than one diameter. A hard-sphere repulsion may be approximated by a reflecting boundary condition at $|\mathbf{r}| = d$ when solving equations such as (47), but there does not seem to be any simple way to enforce inter-particle forces exactly. However, this may be precisely why the model remains mathematically tractable and intuitive, while capturing the essential physics of diffusion in dense flows.

VIII. APPLICATION TO SILO DRAINAGE

A. Statistical Dynamics of Spots

The analysis in the previous section makes no assumptions about spots, other than the existence of well-defined local mean density, mean velocity, and diffusion tensor, which may depend on time and space. As such, the results may have relevance for a variety of dense disordered systems exhibiting cooperative diffusion (see below). In this section, we apply the general theory to the specific case of granular drainage, in which spots diffuse upward from a silo orifice.

For simplicity, let us assume that each spot undergoes mathematical Brownian motion with a vertical drift velocity, $\mathbf{u}_s = v_s \hat{z}$, and a diagonal diffusion tensor,

$$\mathbf{D}_s = \begin{pmatrix} D_s^\perp & 0 & 0 \\ 0 & D_s^\perp & 0 \\ 0 & 0 & D_s^\parallel \end{pmatrix} \quad (48)$$

which allows for a different diffusivity in the horizontal (\perp) and vertical (\parallel) directions due to the symmetry-breaking effect of gravity. In that case, the propagator for a single “spot tracer”, $P_s(\mathbf{x}, z, t | \mathbf{x}_0, z_0, t)$, satisfies another Fokker-Planck equation,

$$\frac{\partial P_s}{\partial t} + \frac{\partial}{\partial z} (v_s P_s) = \nabla_\perp^2 (D_s^\perp P_s) + \frac{\partial^2}{\partial z^2} (D_s^\parallel P_s). \quad (49)$$

The coefficients may depend on space (e.g. larger velocity above the orifice than near the stagnant region), as suggested by the experimental density-wave measurements discussed above [106].

The geometrical spot propagator, $\mathcal{P}_s(\mathbf{x}, |z, \mathbf{x}_0, z_0)$, is the conditional probability of finding a spot at horizontal

position \mathbf{x} once it has risen to a height z from an initial position (\mathbf{x}_0, z_0) . For constant v_s and \mathbf{D}_s , the geometrical propagator satisfies the diffusion equation,

$$\frac{\partial \mathcal{P}_s}{\partial z} = b \nabla_\perp^2 \mathcal{P}_s \quad (50)$$

where $b = D_s^\perp v_s$ is the kinematic parameter. If spots move independently, this equation is also satisfied by the steady-state mean spot density, $\rho_s(\mathbf{x}, z)$, analogous to Eq. (4) for the void density in the Void Model. However, the mean particle velocity in the Spot Model, Eq. (33), is somewhat different, as it involves nonlocal effects (see below).

The time-dependent mean density of spots, $\rho_s(\mathbf{x}, z, t)$, depends on the mean spot injection rate, $Q(\mathbf{x}_0, z_0, t)$ (number/area \times time), which may vary in time and space due to complicated effects such as arching and jamming near the orifice. It is natural to assume that spots are injected at random points along the orifice (where they fit) according to a space-time Poisson process with mean rate, Q . In that case, if spots do not interact, the spatial distribution of spots within the silo at time t is also a Poisson process with mean density,

$$\rho_s(\mathbf{x}, z, t) = \int d\mathbf{x}_0 \int dz_0 \int_{t_0 < t} dt_0 Q(\mathbf{x}_0, z_0, t) P_s(\mathbf{x}, z, t | \mathbf{x}_0, z_0, t_0). \quad (51)$$

For a point-source of spots (i.e. an orifice roughly one spot wide) at the origin with flow rate, $Q_0(t)$ (number/time), this reduces to

$$\rho_s(\mathbf{x}, z, t) = \int_{t_0 < t} dt_0 Q_0(t_0) P_s(\mathbf{x}, z, t | 0, 0, t_0), \quad (52)$$

where P_s is the usual Gaussian propagator for Eq. (49) in the case of constant u_s and \mathbf{D}_s . In reality, spots should weakly interact, but the success of the Kinematic Model suggests that spots diffuse independently as a good first approximation.

B. Statistical Dynamics of Particles

Integral formulae for the drift velocity and diffusivity tensor of a tracer particle may be obtained by substituting the spot density which solves Eq. (51) into the general expressions (33) and (37), respectively. For example, if spots only diffuse horizontally ($D_s^\parallel = 0$), then the mean downward velocity of particles is given by

$$v_p(\mathbf{r}, t) = \int dV_s w(\mathbf{r}_p, \mathbf{r}_s) \rho_s(\mathbf{r}_s, t) v_s(\mathbf{r}_s, t) \quad (53)$$

The main difference with the analogous prediction of the Void Model, Eq. (5), is the convolution with the spot influence function. These sorts of integrals are most important in regions of high shear, where the spot density

and/or spot dynamics varies on scales comparable the spot size (several particles wide).

For simplicity, let us consider a bulk region where the spot density varies on scales much larger than the spot size. In this limit, the integrals over the spot influence function reduce to the following “interaction volumes”:

$$V_k(\mathbf{r}) = \int d\mathbf{r}_s w(\mathbf{r}, \mathbf{r}_s)^k \quad (54)$$

for $k = 1, 2$. (Note that $V_1 = V_s$ above.) The equation for tracer-particle dynamics (30) then takes the form,

$$\begin{aligned} \frac{\partial P_p}{\partial t} = & \frac{\partial}{\partial z} \left[\left(v_s \rho_s - 2D_s^\parallel \frac{\partial \rho_s}{\partial z} \right) V_1 P_p \right] \\ & - 2\nabla_\perp \cdot (D_s^\perp (\nabla_\perp \rho_s) V_1 P_p) \\ & \frac{\partial^2}{\partial z^2} (D_s^\parallel \rho_s V_2 P_p) + \nabla_\perp^2 (D_s^\perp \rho_s V_2 P_p). \end{aligned} \quad (55)$$

Again, it is clear that rescaling the spot density is equivalent to rescaling time.

When the spot dynamics is homogeneous (i.e. u_s and D_s are constants), Equation (55) simplifies further:

$$\begin{aligned} \frac{1}{v_s V_s} \frac{\partial P_p}{\partial t} = & \left(\frac{\partial}{\partial z} + b_p^\perp \nabla_\perp^2 + b_p^\parallel \frac{\partial^2}{\partial z^2} \right) (\rho_s P_p) \\ & - 2b^\perp \nabla \cdot (P_p \nabla \rho_s) - 2b^\parallel \frac{\partial}{\partial z} \left(P_p \frac{\partial \rho_s}{\partial z} \right) \end{aligned} \quad (56)$$

where $b^\perp = b = D_s^\perp / v_s$ and $b^\parallel = D_s^\parallel / v_s$ are the spot diffusion lengths and $b_p^\perp = b_p V_2 / V_1$ and $b_p^\parallel = b^\parallel V_2 / V_1$ are the particle diffusion lengths. In this approximation, the latter are given by the simple formula,

$$\frac{b_p^\perp}{b^\perp} = \frac{b_p^\parallel}{b^\parallel} = \frac{\int dV_s w(\mathbf{r}, \mathbf{r}_s)^2}{\int dV_s w(\mathbf{r}, \mathbf{r}_s)} \quad (57)$$

which generalizes Eqs. (11) and (23) derived above for a uniform spot with a sharp cutoff. In the case of a Gaussian spot, Eq. (43), we obtain a simple relation,

$$\frac{b_p^\perp}{b^\perp} = \frac{b_p^\parallel}{b^\parallel} = \frac{V_s}{8\pi^{3/2}\sigma^3} \quad (58)$$

between the particle and spot diffusion lengths and the spot size and free volume.

The physical meaning of the diffusion lengths becomes more clear in the limit of uniform flow, $\rho_s = \text{constant}$. In terms of the position in a frame moving with the mean flow, $\zeta = v_p t - z$, where $v_p = v_s V_s \rho_s$, we arrive at a simple diffusion equation,

$$\frac{\partial P_p}{\partial \zeta} = \left(b_p^\perp \nabla_\perp^2 + b_p^\parallel \frac{\partial^2}{\partial \zeta^2} \right) P_p, \quad (59)$$

where ζ acts like time. Therefore, b_p^\perp and b_p^\parallel are the variances of the displacements in the perpendicular and parallel directions per twice the mean distance dropped.

Solutions to the new equations above and comparisons with experimental data are left for future work.

IX. OUTLOOK FOR GRANULAR MATERIALS

A. Silo Drainage as a Physics Problem

Gravity-driven silo drainage is an ideal system for fundamental studies of diffusion and mixing. The simplicity of the setup, free of externally applied shear, rotation, or vibration, may make it the easiest to understand in microscopic detail. Future work should focus on detailed comparisons between the present theory (both discrete models and continuum equations), experiments, and granular dynamics simulations. It is natural to start with dry, cohesionless, monodisperse grains, as in this work, and then move on to more complicated granular materials. Surely many more physical principles remain to be discovered. An important goal should be connect with an appropriate continuum model, perhaps among those cited in the introduction. Few of these models have been carefully tested in silo-drainage experiments, and none has been derived systematically from a microscopic theory including diffusion.

One such model, due to Aranson *et al.* [58, 59] postulates the co-existence of “liquid-like” and “solid-like” micro phases in the granular flow, where the local liquid fraction is an order parameter following *ad hoc* Landau-type dynamics. (This is a substantial generalization of models of surface avalanches, which postulate co-existing static and rolling phases [120, 121], and bears some similarity to models of the glass transition [95, 122].) The length scale for order-parameter variations is assumed to be of order the particle diameter, even though this might seem too small for a continuum theory of co-existing phases.

In spite of its successes in describing experimental flows, the order parameter lacks any clear microscopic basis. The present work, however, suggests that it may be related to the spot density, at least in the case of silo drainage (which has not yet been analyzed). If a successful connection could be made with statistical dynamics, it would be reminiscent of the microscopic theory of superconductivity, which came decades after the phenomenological macroscopic description of Ginzburg and Landau [58]. Such connections may also exist with other empirical continuum theories of granular and glassy systems, which invoke the “free volume per atom” as a sort of order parameter controlling material response.

B. Some Open Questions about Spots

There are many questions about silo drainage raised by this work, once one accepts the existence of spots. *How do spots move?* Does their drift velocity, diffusivity, and/or shape depend on particle properties, position in the silo, or the presence of other spots? How do spots interact with container walls or free surfaces? *How do particles move within spots?* What are the “extra” fluctuations associated with small-scale super-diffusion and

the strict enforcement of packing constraints? Does the spot influence depend on the local velocity, shear rate, or stress, the friction and elasticity of the particles, etc.? *How do spots interact?* What kind of attraction and repulsion between spots is responsible for stabilizing the volume fraction in the range of flowing random packings? Do spots subdivide and recombine? *How are spots created and destroyed?* How do spots behave at an orifice or free surface? How do dilation and compaction create and destroy spots in the bulk?

Even more basic questions have to do with the foundations of the theory. *Why do spots even exist?* In a general sense, cooperative motion arises from strong dissipation in the presence of packing constraints (as in gravitational inelastic collapse [10, 123]), but why should the motion be driven by coherent spots of free volume as described here? This motivates the question of whether spot properties can be predicted from first principles. If so, what are the key ingredients of a complete *ab initio* theory? It seems that spots are mainly a consequence of geometrical constraints in flowing, dense random packings, but this connection should be made more precise. The statistical geometry of random packings [11] may be an appropriate starting point.

C. Other Gravity Driven Flows

Since there is strong evidence for spots in silo drainage, it is natural to assume they also exist in other gravity-driven flows. In the case of flow down an inclined chute [124], cooperative motion has also been invoked, albeit without a precise microscopic description. Ertaş and Halsey have explained the Bagnold scaling of the mean velocity in terms of “granular eddies”: coherent structures, several particles in diameter, which rotate rigidly in the same sense (as if rolling down the plane) [123]. However, no evidence for granular eddies has yet been found in experiments or granular dynamics simulations [102].

The basic argument for granular eddies [123] could also be made for spots: Strong dissipation (“gravitational collapse” [10]) causes particles to move cooperatively with their nearest neighbors. Perhaps some composite picture is appropriate for chute flows, although internal rotation with the shear may not be necessary. With simple spots, shear can occur, as in the flow region in a draining silo, when there is a gradient in the spot density transverse to the mean spot drift. With a theory of how spots interact with the free surface, it may be possible to explain the data without including internal same-sense rotations (or eddies) in the Spot Model.

In the context of similar experiments in an inclined pipe [57], Pouliquen *et al.* have proposed a totally different mechanism for dense shear flow [56]. They postulate that flow occurs by a nonlocal fluctuation-activated process: A shear event in one location initiates stress fluctuations which can trigger or enhance shear in another

location by exceeding a local Coulomb yield criterion. A simple probabilistic model of this process describes the experimental mean flow across the pipe cross section fairly well, but the microscopic picture based on single-particle hopping into “holes” seems dubious, in light of the present work. (“A particle... will jump to the next hole with a probability equal to the probability that the stress fluctuation is higher than the threshold” [56].) As in the Void Model for drainage, this picture should not be taken literally since cooperative motion is likely to occur. Perhaps, instead, a spot is triggered to move in the opposite direction by stress fluctuations in response to other spot displacements. Such interactions are not considered in the present model and might be important in more general situations.

D. Forced Shear Flows

Shear flows can also be driven by moving rough surfaces in granular Couette cells [65]. Such forced shear flows seem quite different from the gravity-driven flows discussed above, but some similarities arise, which could be signs of the sort of cooperative diffusion described here. It is usually found that the shear usually localizes in a narrow band at the inner cylinder, as in some pipe flows, but recently broad shear bands have also been observed by Fenistein and van Hecke [125]. If outer part of the lower wall rotates with the outer cylinder while the inner part remains fixed with the inner cylinder, then a region of shear smoothly connects stagnant regions on either side of the interface. Rising through the Couette cell, the shear region broadens and then drifts toward the inner cylinder where it eventually localizes.

The situation is reminiscent of the broad flow region in silo drainage, aside from the direction of the velocity (in the horizontal plane of rotation). In both cases, the velocity profile has a self-similar form reminiscent of diffusion problems. In the Couette flow, it is an error function, as if connecting two uniform concentrations, rather than a Gaussian (for a point source). Unlike gravity-driven drainage, the scaling of the shear zone is not that of simple diffusion, since its width grows somewhat faster than the square root of height, prior to localization near the inner cylinder. Nevertheless, it may be that some kind of spot-like cooperative diffusion originating with dilation at the shearing interface and propagating upward may explain the velocity profile of the shear band.

E. Statistical Thermodynamics of Dense Flows?

As discussed in the introduction, classical statistical thermodynamics does not apply to slow granular flows, because the usual definition of temperature, in terms of undissipated internal energy, makes no sense. In the opposite limit of static granular systems, some radically different definitions have been proposed. For example,

Ngan’s “mechanical temperature” attempts to describe frozen configurational entropy in terms of contact-force distributions [25].

Edwards’ thermodynamic theory of granular compaction [9, 71, 72, 73] focuses instead on excess volume and is thus closer in spirit to the Spot Model. His basic assumption is that all jammed configurations at a given volume are equally probable. This form of ergodicity is analogous to Boltzmann’s famous postulate that all states at a given energy are equally probable.

Following this analogy, Edwards defines the “compactivity”, analogous to temperature, as the derivative of volume with respect to entropy (number of jammed configurations). The compactivity can also be related to volume fluctuations, e.g. as measured in vibrational experiments [75], just as the usual temperature is related to velocity fluctuations. Recent granular simulations have demonstrated an effective Einstein relation in bulk shear flows, where the “temperature”, defined as the ratio of the diffusivity to the mobility (in response to a force pulling on one grain), is consistent with the Edwards compactivity [67]. This suggests that the Edwards ensemble may have relevance for dense flows, although it is not clear how to predict the diffusivity or derive equations for hydrodynamics.

It is tempting to speculate that the spot density in silo drainage is somehow related to the Edwards temperature (or compactivity). Indeed, the diffusivity of particles is proportional to the spot density, so the Spot Model distinguishes between a “warm” region of fast dynamics and “cold” region of slow dynamics by the amount of free volume. This also seems consistent with viewing the compactivity as an intensive variable controlling diffusion.

The drift of particles, however, is also proportional to the spot density, and thus, if the analogy were correct, to temperature. This troubling implication, which violates the notion of “temperature” as a measure of fluctuations, is related to the experimental fact that fluctuations depend on the distance dropped, not time [37]. The reader may conclude that any attempt at a thermodynamic description of dense granular flows is unlikely to succeed.

On the other hand, the Spot Model may provide a basis for some kind of thermodynamics. Rather than describing the system of strongly interacting particles, which is wrought with difficulties related to geometrical packing constraints, perhaps we should consider a system of weakly interacting spots. We have already seen that this gives a simple explanation of density waves, but perhaps it could also be used to recover thermodynamics. The spot diffusivity would be determined by a “spot temperature” (perhaps related to the Edwards definition) and the spot drift by independent external forcing due to gravity. Even if spots were to obey classical statistical mechanics (starting from a “spot Hamiltonian”), the particles would behave rather differently, with drift strongly coupled to diffusion.

F. Compaction Dynamics

Even in the absence of flow, granular materials exhibit nontrivial relaxation phenomena, such as compaction (or densification) under vibration. Experiments on vertically vibrated granular materials have revealed a very slow $(\log t)^{-1}$ decay of free volume with time [75, 126]. To explain this result, Bouteux and de Gennes [127] borrow classical equations from glass theory, due to Cohen and Turnbull [95] (see below): (i) They assume a Poisson distribution of “holes” of volume V ,

$$p(V) = \frac{1}{V_f} e^{-V/V_f} \quad (60)$$

where V_f is the local “free volume”, defined (albeit ambiguously [11, 14, 15]) so that $V_f = 0$ in the hypothetical “random close packing”. (ii) The empirical relation, $V_f \propto (\log t)^{-1}$, then follows from the mean-field assumption that the rate of compaction, dV_f/dt , is proportional to the probability

$$P(V_0) = e^{-V_0/V_f} \quad (61)$$

of finding a hole larger than a particle volume, V_0 . Such a hole, capable of being filled by a single particle, corresponds to a “void” [75].

This thinking reflects the entrenched notion that structural rearrangement in an amorphous material occurs by the independent displacement of a particle into a randomly appearing void. Unlike hypothetical voids in granular drainage, which propagate by exchanging places with particles, those in granular compaction are annihilated by hopping particles. This picture of compaction has been compared to the “parking-lot model” of cars trying to fill a dwindling set of available spaces [75].

We have shown that voids do not play a significant role in dense granular drainage, so it seems unlikely that they could also occur in compaction dynamics, which occurs at ever higher volume fractions, closer to the jammed state. We would also expect nearest-neighbor cages to remain largely preserved during compaction, especially in the later stages, when the density is much closer to the jammed state than in the drainage flows considered here (which exhibit very slow cage breaking). It seems more plausible that particles rearrange in a cooperative fashion during compaction, slowly eliminating interstitial free volume without ever opening any particle-sized voids.

The Spot Model provides a general theoretical framework to describe such collective mechanisms for transporting free volume from the bulk to the upper surface. Note that a new microscopic mechanism need not contradict the prior successes of mean-field free-volume models. As with the mean velocity of granular drainage, the mean compaction rate could be very similar with spots and voids, even though diffusion and cage-breaking are completely different in the two cases. The characteristic free volume, v_0 , in Eq. (61) should be related to the typical volume carried by a spot, which is roughly a tenth

of a particle volume in granular drainage. This is consistent with the more general view of v_0 as the “typical free-volume fluctuation required for a local collapse” (see below) [60].

X. OUTLOOK FOR GLASSES

A. Glassy Relaxation

A major reason for the current excitement about granular materials in physics is the analogy with glasses, which exhibit similar features such as “structural temperatures” [74] and a “jamming transition” [17]. The hope is that such common features could shed light on the nature of glass and the glass transition [128], which has been called “the deepest and most interesting unsolved problem in solid state theory” [129]. As in the case of granular flow, many toy models and continuum approaches have been proposed, but glassy relaxation remains poorly understood at the microscopic level.

It has long been recognized that cooperative motion plays a crucial role in glassy relaxation, although precise mechanisms remain elusive. Early theories of the diverging relaxation time at the glass-transition temperature [130, 131] were based on the hypothesis of free-volume diffusion [95, 96, 132, 133]. Adam and Gibbs first suggested instead that free volume is associated with temperature-dependent regions of cooperative relaxation, whose size diverges at the glass transition [134]. Cohen and Grest later introduced more explicit correlations into free-volume theory (see below) by considering clusters of “liquid-like cells”, so the melting of glass could be understood as a dynamical percolation transition [122]. The mode-coupling theory of Götze and Sjögren has invoked the “cage effect” of local blocking at the scale of single particles to explain the emergence of slow dynamics [135], albeit without describing how it occurs in real space. In contrast, Berthier has provided new simulation evidence for the Adam-Gibbs hypothesis that the glass transition is associated with dynamical correlations at a length scale which grows with decreasing temperature [136].

Experiments and simulations have revealed ample signs of “dynamical heterogeneity” in supercooled liquids and spin glasses [137], but the direct observation of cooperative motion has been achieved only recently. Rather than compact regions of local arrangement, Donati *et al.* have observed “string-like” relaxation in molecular dynamics simulations of a Lennard-Jones model glass [138]. The strength and length scale of correlations increases with decreasing temperature [139], consistent with the Adam-Gibbs hypothesis. These observations have motivated Garrahan and Chandler to propose a phenomenological lattice model where each site possesses an arrow pointing in the “mean direction of facilitation” (opposite to the preferred direction of flow) and chain-like relaxation follows from dynamical interactions between the

arrows [140]. (The idea of a local vector state variable also arises in theories of plasticity, discussed below.)

Cooperative motion would be difficult to observe experimentally in a molecular glass, but Weeks *et al.* have used confocal microscopy to reveal three-dimensional clusters of fast-moving particles in dense colloids [141]. In the supercooled liquid, clusters of cooperative relaxation have widely varying sizes, which grow as the glass transition is approached. In the glass phase, the clusters are much smaller, on the order of ten particles, and do not produce significant rearrangements on experimental time scales.

These observations suggest that spots may have relevance for cooperative diffusion in simple glasses. String-like relaxation is reminiscent of the trail of a spot (see Fig. 6). Atomic chains would correspond to the motion of spots roughly one particle in size and carrying less than one particle of free volume. Larger regions of correlated motion might involve larger spots and/or collections of interacting spots. Key features of the experimental data [141] seem to support this idea: (i) Correlations take the form of “neighboring particles moving in parallel directions” (as in Fig. 7); and (ii) the large clusters of correlated motion tend to be fractals with dimension two, as would be expected for the random-walk trail of a spot (as in Fig. 6 without the bias of gravity). It seems more experiments and simulations should be done to test the spot hypothesis for various glass-forming systems.

B. Free-Volume Theory

For metallic glasses [142, 143], free-volume theory provides the basis for modern continuum models of plastic flow and diffusion. The concept of hole diffusion was apparently introduced in 1936 by Eyring [96], but Cohen and Turnbull in 1959 initiated the standard model of glassy relaxation [95, 144, 145], based on Eqs. (60) and (61). In their theory of “molecular transport in liquids and glasses” (on the same footing), randomly distributed “holes” are filled by single-particle displacements, whenever a hole is large enough to accommodate a neighboring particle, with probability $P(v_0) = e^{v_0/v_f}$. These assumptions yield the classical formula, $D \propto e^{-v_0/v_f}$, for the diffusivity, where a linear dependence of free volume on temperature, $v_f = A + B(T - T_g)$, above the glass transition, T_g , is commonly assumed, as suggested by Williams, Landel, and Ferry [131]. By assuming that hole diffusion is biased by the local shear stress, Spaepen derived Doolittle’s formula for the viscosity, $\eta \propto e^{v_0/v_f}$, and proposed mechanisms for the creation and annihilation of free volume based on particles jumping into holes of a smaller or larger volume, respectively [146].

Of course, this microscopic picture is very similar to that of the Void Model for granular drainage, where gravity provides a bias for void diffusion (so voids are created at the orifice and destroyed at the free surface). Indeed, Spaepen’s Figure 3 [146] is nearly identical to Figure 2

above. The key point is that, in both cases, flow and diffusion occur when a single particle moves into a void independently from its neighbors.

Since cooperative diffusion is widely believed to occur in glasses, the Spot Model seems to provide a more realistic mechanism for free volume diffusion. As we have demonstrated for granular drainage, this could be checked in glasses by comparing the diffusion lengths for free volume and particles and the cage-breaking length (which must all be roughly the same for hole diffusion) or by directly observing spatial velocity correlations. If interacting spots exist in metallic glasses, perhaps they are responsible for the formation of shear bands of reduced density under large tensile loading [147]. Shear bands in metallic glasses are difficult to understand, because, unlike shear bands in crystals, which are known to result from dislocation interactions, it is not clear what are the microscopic carriers of plastic deformation in disordered materials.

C. Plastic Deformation

The idea of localized cooperative motion has a long history in the plastic deformation of amorphous solids. Orowan [148] was perhaps the first to propose, contrary to Eyring’s hole-diffusion hypothesis, that plastic flow occurs via localized shear transformations in regions of enhanced atomic disorder (and free volume) [148]. In the context of metallic glasses, Argon [149] later distinguished between two types of local rearrangements: (i) a “diffuse shear transformation” at high temperature, in which a spherical region 4-6 atoms in diameter deforms smoothly into an ellipsoidal shape, and (ii) an “intense shear transformation” at low temperature, in which an equally small disk-shaped region, similar to a dislocation loop, slides suddenly along an atomic slip plane. A generalization of this concept, the “localized inelastic transformation” (LIT), forms the basis of a stochastic model of elasto-plastic deformation due to Bulatov and Argon [150]. Each LIT acts irreversibly on a material element as a pure shear along some discrete axis of symmetry plus an additional dilation.

The basic idea of the LIT has recently been revived in physics [151] as a “shear transformation zone” (STZ) [152], connecting “+” and “-” states relative to the direction of an applied shear. Falk and Langer first identified STZ events in molecular dynamics simulations of a Lennard-Jones glass and proposed a new continuum theory of viscoplastic deformation, which involves the densities, n_{\pm} , of the two hypothetical STZ types as auxiliary continuum variables (or order parameters) [152]. They noted that STZ transition rates should depend on the local free volume, taken to be constant as a first approximation. STZ theory compares favorably with experimental data on metallic glasses [153], although it contains a number of adjustable parameters and *ad hoc* functional forms.

Lemaître has recently extended the two-state STZ theory to account for the creation and annihilation (but not diffusion) of free volume [60], borrowing some equations from the literature on metallic glasses and granular compaction discussed above. The resulting empirical constitutive laws are meant to apply to a broad class of sheared dense materials, including glasses [154] and granular materials [61]. The same phenomenology provides a fairly simple way of understanding universal features of amorphous systems, such as stick-slip, dilatancy, and nonlinear rheology, although again the microscopic mechanisms remain vague. Moreover, if free volume is created and destroyed by particle displacements, it seems it should also diffuse by very similar mechanisms (as in Spaepen’s theory [146]).

Although neglecting diffusion, Lemaître offers a new, qualitative interpretation of free-volume kinetics, of particular interest here: “Borrowing on the argument of STZ theory, compaction results from elementary rearrangements, involving several molecules at the mesoscopic scale”, rather than “the motion of a single grain in a hole” [154]. Of course, we have reached the same conclusion in the completely different context of granular flow. Lemaître gives no further description of the “elementary rearrangements” associated with free-volume dynamics, but the Spot Model provides a possible mathematical framework, which also naturally accounts for diffusion. This seems like an interesting direction for future research.

XI. CONCLUSION

Returning to our original question about random walks, we arrive at a simple *dynamical* distinction between different states of matter:

Gas. The particles in a gas undergo independent random walks, as ballistic trajectories are randomly redirected by collisions.

Crystal. The particles in a (single) crystal diffuse by hopping to either interstitial or vacant lattice sites. Both interstitials and vacancies undergo thermally activated, independent random walks on the lattice (at sufficiently low defect density).

Liquid. The particles in a liquid move cooperatively at the scale of several particles, but, due to the high internal kinetic energy, they undergo independent random walks over much longer distances at experimental time scales.

Amorphous. The particles in an amorphous state move cooperatively at experimental time scales, due to the low internal energy. Proximity to jamming precludes the vacancy/interstitial mechanism (inserting particles into holes). Instead, particles undergo locally correlated random walks in response to diffusing spots of free volume.

This is surely an oversimplification. For example, directional covalent bonding can significantly alter the picture: In amorphous silicon, vacancy (dangling bond [155]) or interstitial (floating bond [156]) mechanisms may dominate relaxation, while in open lattices like diamond silicon, cooperative self-diffusion can also occur (concerted exchange [157]). Nevertheless, for materials with dense disordered phases, the state classification above by diffusion mechanism seems reasonable.

In summary, the Spot Model provides a simple mathematical framework for cooperative diffusion, when independent random walks are inhibited by packing constraints. Like the original random-walk concept, which is now used in many fields other than physics, the basic idea of a moving “spot of influence” may also have

broader applications.

Acknowledgements

This work was supported by the U. S. Department of Energy (grant DE-FG02-02ER25530) and the Norbert Wiener Research Fund and NEC Fund at MIT. The author is grateful to J. Choi, C. Guáqueta, A. Kudrolli, R. R. Rosales, C. H. Rycroft, and A. Samadani for providing figures of unpublished results and for many stimulating discussions, and to A. S. Argon, L. Bocquet, M. Demkowicz, R. Raghavan for references to the glass literature.

-
- [1] R. M. Nedderman, *Statics and Kinematics of Granular Materials* (Cambridge University Press, 1992).
 - [2] A. Schofield and C. Wroth, *Critical State Soil Mechanics* (McGraw-Hill, New York, 1968).
 - [3] R. C. Brown and J. C. Richards, *Principles of Powder Mechanics* (Pergamon, New York, 1970).
 - [4] H. M. Jaeger and S. R. Nagel, *Science* **255**, 1523 (1992).
 - [5] A. Mehta and G. C. Barker, *Rep. Prog. Phys.* **57**, 383 (1994).
 - [6] H. M. Jaeger, S. R. Nagel, and R. P. Behringer, *Rev. Mod. Phys.* **68**, 1259 (1996).
 - [7] P. G. de Gennes, *Rev. Mod. Phys.* **71**, S374 (1999).
 - [8] T. Halsey and A. Mehta, eds., *Challenges in Granular Physics* (World Scientific, 2002).
 - [9] S. F. Edwards and D. V. Grinev, *Advances in Complex Systems* **4**, 451 (2001), (also reprinted in Ref. [8]).
 - [10] L. P. Kadanoff, *Rev. Mod. Phys.* **71**, 435 (1999).
 - [11] S. Torquato, *Random Heterogeneous Materials* (Springer, New York, 2002).
 - [12] S. Torquato and F. H. Stillinger, *J. Phys. Chem. B* **106**, 8354 (2002).
 - [13] A. J. Liu and S. R. Nagel, *Nature (London)* **396**, 21 (1998).
 - [14] S. Torquato, T. M. Truskett, and P. G. Debenedetti, *Phys. Rev. Lett.* **84**, 2064 (2000).
 - [15] A. R. Kansal, S. Torquato, and F. H. Stillinger, *Phys. Rev. E* **66**, 041109 (2002).
 - [16] C. S. O'Hern, S. A. Langer, A. J. Liu, and S. R. Nagel, *Phys. Rev. Lett.* **88**, 075507 (2002).
 - [17] C. S. O'Hern, L. E. Silbert, A. J. Liu, and S. R. Nagel, *Phys. Rev. E* **68**, 011306 (2003).
 - [18] S. Torquato and F. H. Stillinger, *J. Phys. Chem. B* **105**, 11849 (2001).
 - [19] J.-P. Bouchaud, M. E. Cates, and P. Claudin, *J. Phys.* **5**, 639 (1995).
 - [20] S. N. Coppersmith, C. h. Liu, S. Majumdar, O. Narayan, and T. A. Witten, *Phys. Rev. E* **53**, 4673 (1996).
 - [21] D. M. Mueth, H. M. Jaeger, and S. R. Nagel, *Phys. Rev. E* **57**, 3164 (1998).
 - [22] D. L. Blair, N. Mueggenburg, A. M. Marshall, H. M. Jaeger, and S. R. Nagel, *Phys. Rev. E* **63**, 041304 (2001).
 - [23] J. W. Landry, G. S. Grest, L. E. Silbert, and S. J. Plimpton, *Phys. Rev. E* **67**, 041303 (2003).
 - [24] S. F. Edwards, *Physica A* **249**, 226 (1998).
 - [25] A. H. W. Ngan, *Phys. Rev. E* **68**, 011301 (2003).
 - [26] S. B. Savage, *J. Fluid Mech.* **92**, 53 (1979).
 - [27] S. B. Savage and D. J. Jeffrey, *J. Fluid Mech.* **110**, 255 (1981).
 - [28] J. T. Jenkins and S. B. Savage, *J. Fluid Mech.* **130**, 187 (1983).
 - [29] P. K. Haff, *J. Fluid Mech.* **134**, 187 (1983).
 - [30] C. K. K. Lun, S. B. Savage, D. J. Jeffrey, and N. Chepur, *J. Fluid Mech.* **140**, 223 (1984).
 - [31] S. S. Hsiao and M. L. Hunt, *J. Heat Transfer* **115**, 541 (1993).
 - [32] J. W. Dufty, *Advances in Complex Systems* **4**, 397 (2001), (also reprinted in Ref. [8]).
 - [33] J. R. Prakash and K. K. Rao, *J. Fluid Mech.* **225**, 21 (1991).
 - [34] C. Tsallis, *J. Stat. Phys.* **52**, 479 (1988).
 - [35] F. Sattin, *J. Phys. A* **36**, 1583 (2003).
 - [36] V. V. R. Natarajan, M. L. Hunt, and E. D. Taylor, *J. Fluid Mech.* **304**, 1 (1995).
 - [37] J. Choi, A. Kudrolli, R. R. Rosales, and M. Z. Bazant, *Phys. Rev. Lett.* **92**, 174301 (2004).
 - [38] W. G. Pariseau, *Powder Technology* **3**, 218 (1970).
 - [39] P. M. Blair-Fish and P. L. Bransby, *J. Eng. Ind. Trans. ASME, Ser. B* **95**, 17 (1973).
 - [40] R. L. Michalowski, *Powder Technology* **39**, 29 (1984).
 - [41] A. Medina, J. A. Cordova, E. Luna, and C. Trevino, *Physics Letters A* **220**, 111 (1998).
 - [42] A. Samadani, A. Pradhan, and A. Kudrolli, *Phys. Rev. E* **60**, 7203 (1999).
 - [43] R. M. Nedderman and U. Tüzün, *Powder Technology* **22**, 243 (1979).
 - [44] U. Tüzün and R. M. Nedderman, *Powder Technology* **23**, 257 (1979).
 - [45] D. G. Schaeffer, *J. Diff. Eq.* **66**, 19 (1987).
 - [46] E. B. Pitman and D. G. Schaeffer, *Commun. Pure. Appl. Math.* **40**, 421 (1987).
 - [47] J. Mullins, *Powder Technology* **9**, 29 (1974).
 - [48] J. Litwiniszyn, *Rheol. Acta* **2/3**, 146 (1958).
 - [49] J. Litwiniszyn, *Bull. Acad. Pol. Sci.* **9**, 61 (1963).
 - [50] J. Litwiniszyn, *Bull. Acad. Pol. Sci.* **11**, 593 (1963).

- [51] J. Mullins, J. Appl. Phys. **43**, 665 (1972).
- [52] S. B. Savage, J. Fluid Mech. **377**, 1 (1998).
- [53] L. Bocquet, W. Losert, D. Schalk, T. C. Lubensky, and J. P. Gollub, Phys. Rev. E **65**, 011307 (2002).
- [54] W. Losert, L. Bocquet, T. C. Lubensky, and J. P. Gollub, Phys. Rev. Lett. **85**, 1428 (2000).
- [55] P. Mills, D. Loggia, and M. Tixier, Europhys. Lett. **45**, 733 (1999).
- [56] O. Pouliquen, Y. Forterre, and S. L. Dizes, Advances in Complex Systems **4**, 441 (2001), (also reprinted in Ref. [8]).
- [57] O. Pouliquen and R. Gutfraind, Phys. Rev. E **53**, 552 (1996).
- [58] I. S. Aranson and L. S. Tsimring, Phys. Rev. E **64**, 020301 (2001).
- [59] I. S. Aranson, L. Tsimring, and V. M. Vinokur, Phys. Rev. E **60**, 1975 (1999).
- [60] A. Lemaître, Phys. Rev. Lett. **89**, 195503 (2002).
- [61] A. Lemaître, Phys. Rev. Lett. **89**, 064303 (2002).
- [62] S. Horlück and P. Dimon, Phys. Rev. E **60**, 671 (1999).
- [63] S. Horlück and P. Dimon, Phys. Rev. E **63**, 031301 (2001).
- [64] A. Medina, J. Andrade, and C. Trevino, Physics Letters A **249**, 63 (1998).
- [65] D. E. Mueth, G. F. Debregeas, G. S. Karczmar, P. J. Eng, S. R. Nagel, and H. M. Jaeger, Nature **406**, 385 (2000).
- [66] H. A. Makse, N. Gland, D. L. Johnson, and L. M. Schwartz, Phys. Rev. Lett. **83**, 5070 (1999).
- [67] H. A. Makse and J. Kurchan, Nature **415**, 614 (2002).
- [68] D. Hirshfeld and D. C. Rapaport, Eur. Phys. J. E **4**, 193 (2001).
- [69] L. E. Silbert, D. Ertas, G. S. Grest, T. C. Halsey, D. Levine, and S. J. Plimpton, Phys. Rev. E **64**, 051303 (2001).
- [70] L. E. Silbert, D. Ertas, G. S. Grest, T. C. Halsey, and D. Levine, Phys. Rev. E **65**, 031304 (2002).
- [71] S. F. Edwards and D. V. Grinev, Phys. Rev. E **58**, 4758 (1998).
- [72] S. F. Edwards, in *Granular Matter: An Interdisciplinary Approach*, edited by A. Mehta (Springer, 1994).
- [73] S. F. Edwards, in *Disorder in Condensed Matter Physics*, edited by Blackman and Taguena (Oxford, 1991).
- [74] J. Kurchan, Advances in Complex Systems **4**, 363 (2001), (also reprinted in Ref. [8]).
- [75] E. R. Nowak, J. B. Knight, E. Ben-Naim, H. M. Jager, and S. R. Nagel, Phys. Rev. E **57**, 1971 (1998).
- [76] K. Pearson, Nature (London) **72**, 294 (1905).
- [77] Rayleigh, Phil. Mag. **10**, 73 (1880).
- [78] Rayleigh, Nature (London) **72**, 318 (1905).
- [79] A. Einstein, Ann. Physik **17**, 549 (1905).
- [80] M. von Smoluchowski, Ann. Physik **21**, 756 (1906).
- [81] L. Bachelier, Ph.D. thesis, École Normale Supérieure (1900).
- [82] N. Wax, ed., *Selected Papers on Noise and Stochastic Processes* (Dover, New York, 1954).
- [83] B. Hughes, *Random Walks and Random Environments*, vol. 1 (Oxford University Press, 1995).
- [84] J.-P. Bouchaud and M. Potters, *Theory of Financial Risks* (Cambridge University Press, 2000).
- [85] E. W. Montroll and G. H. Weiss, J. Math. Phys. **6**, 167 (1965).
- [86] G. H. Weiss and R. J. Rubin, Advances in Chemical Physics **52**, 363 (1983).
- [87] H. Scher and E. W. Montroll, Phys. Rev. B **12**, 2455 (1975).
- [88] M. F. Schlesinger, B. J. West, and J. Klafter, Phys. Rev. Lett. **58**, 1100 (1987).
- [89] R. Metzler and J. Klafter, Physics Reports **339**, 1 (2000).
- [90] R. Fürth, *Schwankungserscheinungen in der Physik* (Sammlung Vieweg, Braunschweig, 1920).
- [91] G. I. Taylor, Proc. London Math. Soc. **20**, 196 (1921).
- [92] S. Corrsin, *Advances in Geophysics*, vol. 18a (Academic Press, 1974).
- [93] G. H. Weiss, Physica A **311**, 381 (2002).
- [94] J. Mullins, Powder Technology **23**, 115 (1979).
- [95] M. H. Cohen and D. Turnbull, J. Chem. Phys. **31**, 1164 (1959).
- [96] H. Eyring, J. Chem. Phys. **4**, 283 (1936).
- [97] H. Caram and D. C. Hong, Phys. Rev. Lett. **67**, 828 (1991).
- [98] C. Guáqueta, *Computer Simulations of a Stochastic Model for Granular Drainage*, B.S. thesis in Materials Science, MIT (2003).
- [99] W. A. Beverloo, H. A. Leniger, and J. V. de Velde, Chem. Eng. Sci. **15**, 260 (1961).
- [100] M. Z. Bazant, Tech. Rep., MIT Department of Mathematics (2001), cond-mat/0307379/v1.
- [101] J. Choi (private communication), based on the experiments described in Ref. [37].
- [102] J. W. Landry (private communication), based on the granular-dynamics simulation method of Refs. [23, 69].
- [103] G. Y. Onoda and E. G. Liniger, Phys. Rev. Lett. **64**, 2727 (1990).
- [104] O. Pouliquen, M. Nicolas, and P. D. Weldman, Phys. Rev. Lett. **79**, 3640 (1997).
- [105] T. C. Hales, see <http://www.math.pitt.edu/thales> for preprints.
- [106] G. W. Baxter, R. P. Behringer, T. Fagert, and G. A. Johnson, Phys. Rev. Lett. **62**, 2825 (1989).
- [107] S. Torquato and F. H. Stillinger, Phys. Rev. E **68**, 041113 (2003).
- [108] S. Torquato and F. Lado, J. Phys. A **18**, 141 (1985).
- [109] A. Valance and T. L. Pennec, Eur. Phys. J. **5**, 223 (1998).
- [110] G. Ristow and H. J. Herrmann, Phys. Rev. E **50**, R5 (1994).
- [111] J. Lee, Phys. Rev. E **49**, 281 (1994).
- [112] J. Lee and M. Leibig, J. Phys. I France **4**, 507 (1994).
- [113] G. B. Whitham, *Linear and Nonlinear Waves* (Wiley, 1974).
- [114] H. Hayakawa and K. Nakanishi, Progress of Theoretical Physics Supplement **130**, 57 (1998).
- [115] T. Pöschel, J. Phys. (France) I **4**, 499 (1994).
- [116] M. Menon and D. J. Durian, Science **275**, 1920 (1997).
- [117] N. J. Hadjiconstantinou, A. L. Garcia, M. Z. Bazant, and G. He, J. Comp. Phys. **187**, 274 (2003).
- [118] C. H. Rycroft (private communication).
- [119] H. Risken, *The Fokker-Planck Equation* (Springer, 1996).
- [120] J.-P. Bouchaud, M. E. Cates, J. R. Prakash, and S. F. Edwards, J. Phys. I (France) **4**, 1383 (1994).
- [121] T. Boutreux, E. Raphaël, and P.-G. de Gennes, Phys. Rev. E **58**, 4692 (1998).
- [122] M. C. Cohen and G. S. Grest, Phys. Rev. B **20**, 1077

- (1979).
- [123] D. Ertaş and T. C. Halsey, *Europhys. Lett.* **60**, 931 (2002).
 - [124] O. Pouliquen, *Phys. Fluids* **11**, 542 (1999).
 - [125] D. Fenistein and M. van Hecke, *Nature* **425**, 256 (2003).
 - [126] J. B. Knight, C. G. Fandrich, C. N. Lau, H. M. Jaeger, and S. R. Nagel, *Phys. Rev. E* **51**, 3957 (1995).
 - [127] T. Boutreux and P. G. de Gennes, *Physica A* **244**, 59 (1997).
 - [128] C. A. Angell, K. L. Ngai, G. B. McKenna, P. F. McMillan, and S. W. Martin, *J. Appl. Phys.* **88**, 3113 (2000).
 - [129] P. W. Anderson, *Science* **267**, 1615 (1995).
 - [130] H. Vogel, *Physik. Z.* **22**, 645 (1921).
 - [131] M. L. Williams, R. F. Landel, and J. D. Ferry, *J. Am. Chem. Soc.* **77**, 3701 (1955).
 - [132] F. Bueche, *J. Chem. Phys.* **21**, 1850 (1953).
 - [133] T. G. Fox and P. J. Flory, *J. Appl. Phys.* **21**, 581 (1950).
 - [134] G. Adam and J. H. Gibbs, *J. Chem. Phys.* **43**, 140 (1965).
 - [135] W. Götze and L. Sjögren, *Chem. Phys.* **212**, 47 (1996).
 - [136] L. Berthier, cond-mat/0310210.
 - [137] For brief reviews, see Refs. [139], [141], and [136].
 - [138] C. Donati, J. F. Douglas, W. Kob, S. J. Plimpton, P. H. Poole, and S. C. Glotzer, *Phys. Rev. Lett.* **80**, 2338 (1998).
 - [139] C. Donati, S. C. Glotzer, P. H. Poole, W. Kob, and S. J. Plimpton, *Phys. Rev. E* **60**, 3107 (1999).
 - [140] J. P. Garrahan and D. Chandler, *PNAS* **100**, 9710 (2003).
 - [141] E. R. Weeks, J. C. Crocker, A. C. Levitt, A. Schofield, and D. A. Weitz, *Science* **287**, 627 (2000).
 - [142] W. L. Johnson, *MRS Bulletin* **24**, 42 (1999).
 - [143] R. Busch, *JOM* **52**, 39 (2000).
 - [144] D. Turnbull and M. H. Cohen, *J. Chem. Phys.* **34**, 120 (1961).
 - [145] D. Turnbull and M. H. Cohen, *J. Chem. Phys.* **52**, 3038 (1970).
 - [146] F. Spaepen, *Acta Metallurgica* **25**, 407 (1977).
 - [147] This possibility was suggested by R. Raghavan and W. C. Carter.
 - [148] E. Orowan, in *Proceedings of the First International Congress on Applied Mechanics* (AMSE, 1952), p. 453.
 - [149] A. S. Argon, *Acta Metallurgica* **27**, 47 (1979).
 - [150] V. V. Bulatov and A. S. Argon, *Modelling Simul. Mater. Sci. Eng.* **2**, 167 (1994).
 - [151] Compare Fig. 3b of Ref. [149] and Fig. 1 of Ref. [150] with Fig. 8 of Ref. [152] and Fig. 1 of Ref. [60].
 - [152] M. L. Falk and J. S. Langer, *Phys. Rev. E* **57**, 7192 (1998).
 - [153] M. L. Falk, J. S. Langer, and L. Pechenik, cond-mat/0311057.
 - [154] A. Lemaître, cond-mat/0206417.
 - [155] V. M. Burlakov, G. A. D. Briggs, A. P. Sutton, and Y. Tsukahara, *Phys. Rev. Lett.* **86**, 3052 (2001).
 - [156] S. T. Pantelides, *Phys. Rev. Lett.* **57**, 2979 (1986).
 - [157] K. C. Pandey, *Phys. Rev. Lett.* **57**, 2287 (1986).